Small defects reconstruction in waveguides from multifrequency one-side scattering data

Angèle Niclas, L. Seppecher, Eric Bonnetier, Grégory Vial

Small defects reconstruction in waveguides from multifrequency one-side scattering data

Éric Bonnetier[1], Angèle Niclas[2,*], Laurent Seppecher[2], and Grégory Vial[2]

[1]Institut Fourier, Université Grenoble Alpes, France
[2]Institut Camille Jordan, École Centrale Lyon, France
[*]Corresponding author: angele.niclas@ec-lyon.fr

Abstract

Localization and reconstruction of small defects in acoustic or electromagnetic waveguides is of crucial interest in nondestructive evaluation of structures. The aim of this work is to present a new multi-frequency inversion method to reconstruct small defects in a 2D waveguide. Given one-side multi-frequency wave field measurements of propagating modes, we use a Born approximation to provide a L^2-stable reconstruction of three types of defects: a local perturbation inside the waveguide, a bending of the waveguide, and a localized defect in the geometry of the waveguide. This method is based on a mode-by-mode spacial Fourier inversion from the available partial data in the Fourier domain. Indeed, in the available data, some high and low spatial frequency information on the defect are missing. We overcome this issue using both a compact support hypothesis and a minimal smoothness hypothesis on the defects. We also provide a suitable numerical method for efficient reconstructions of such defects and we discuss its applications and limits.

1 Introduction

In this article, we present a method to detect and reconstruct small defects in a waveguide of dimension 2 from multi-frequency wave field measurements. The measurements are made on one section of the waveguide, and we assume that only the propagative modes can be detected. Indeed, in most of the case measurements are made far from the defects where the evanescent modes vanish. In a waveguide $\Omega \subset \mathbb{R}^2$, in the time harmonic regime the wave field u_k satisfies the Helmholtz equation

$$\Delta u_k + k^2(1+q)u_k = -s, \tag{1}$$

where k is the frequency, q is a compactly supported bounded perturbation inside the waveguide and the function s is a source of waves.

We focus on the inversion of three main types of defects represented in Figure 1: a local perturbation of the index q, a bending of the waveguide, and a localized defect in the geometry of Ω. The detection of such defects can be used as a non destructive evaluation to monitor pipes, optical fibers, or train rails for instance (see [15, 14]). A controlled source s generates wave fields in Ω for some frequencies $k \in K \subset \mathbb{R}_+^*$ and we assume the knowledge of the corresponding measurements $u_k(x, y)$ for every $(x, y) \in \Sigma$ where Σ is a section of Ω.

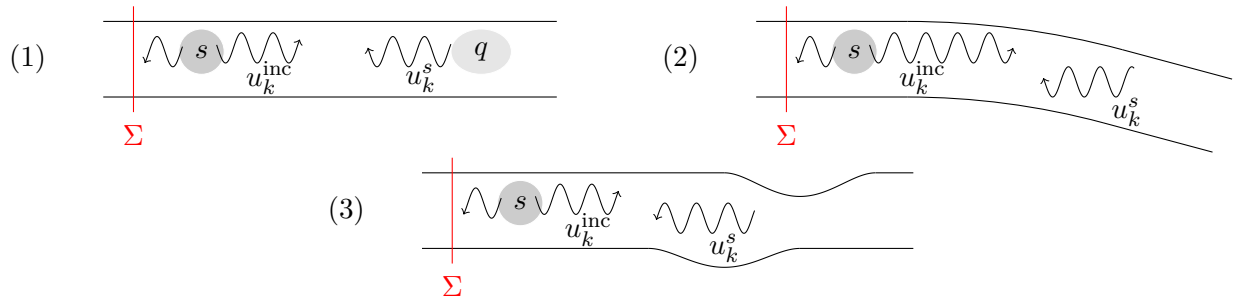

Figure 1: Representation of the three studied types of defects: in (1) a local perturbation q, in (2) a bending of the waveguide, in (3) a localized defect in the geometry of Ω. A controlled source s generates a wave field u_k^{inc}. When it crosses the defect, it generates a scattered wave field u_k^s. Both u_k^{inc} and u_k^s are measured on the section Σ.

The detection of bends or shape defects in a waveguide is mentioned in the articles [16, 2, 1]. To solve the forward problem, the authors use a conformal mapping or a local orthogonal transformation to map the geometry to that of a regular waveguide. This method is very helpful to understand the propagation of waves in irregular waveguides but is hardly adaptable for the inverse problem and for the reconstruction of defects, since the transformation to a regular waveguide is not explicit and proves numerically expensive.

As for the recovery of inhomogeneities in a waveguide using scattered field data, the problem has already been studied by several authors. In [10], the authors use a spectral decomposition and assume the knowledge of the far-field approximation of the scattered wave field to reconstruct the inhomogeneities in a 2D waveguide. The authors in [7] adapt the Linear Sampling Method [8] to waveguides, and detect inhomogeneities in 2D or 3D. In [3], the authors use an asymptotic formula of the scattered field to localize small inclusions. We can also mention [6], where the authors are considering periodic waveguides. In all these articles, the frequency in the Helmholtz equation is fixed and it is assumed that incident waves can be sent on every propagative mode in the waveguide. However, as defects may be invisible at some frequencies (as shown in [11]) the frequency has to be chosen wisely.

Our work concerns a different approach, also used in [4], where we assume that data is available for a whole interval of frequencies. Moreover, we only assume that one can send the first propagative mode in the waveguide as an excitation source. This situation seems closer to the practice of monitoring pipes in mechanical experiments [15]. In this study, we assume that the defects are small in amplitude and/or in support in order to approximate the wave field using its Born approximation. This seems to be a reasonable assumption considering the applications that this work intends to address. This approximation is described in [9], and is also used in [10, 3]. Our strategy to study the impact of small geometrical defects is to provide a well suited mapping from the perturbed waveguide to a perfect waveguide that generates some change in the Helmholtz equation itself. Through the reconstruction of these modifications in the equation while assuming a perfect waveguide, it is possible to recover the defects in the geometry.

An important difficulty in detecting inhomogeneities using one sided multi-frequencies measurements in a waveguide is that low spacial frequency information carried by vanishing modes about the inhomogeneities may be missing. Indeed, these modes are not measurable in practice due to

their exponential decay.

One of the key results of this article is given by Theorem 22 that provides conditions to ensure stable recovery of a function from an incomplete knowledge of its Fourier transform. In this result, we assume that both high frequencies and a reasonable amount of low frequencies are missing. Nevertheless, a stable inversion in L^2 remains possible assuming a reasonable *a priori* knowledge of the smoothness and the support of the unknown perturbation. This result provides a theoretical stability argument that allows us to run a mode-by-mode well-conditioned inversion using a penalized least-squared technique. This method is numerically efficient, and can be applied to recover defects of the three different types.

The paper is organized a follows. In section 2, we recall some properties of the forward source problem in a waveguide using the modal decomposition of both the wave field and the source. We then study the inverse source problem with full frequency data and then with partial frequency data.

In section 3, we apply the results to recover all three types of defects that we are interested in: inhomogeneities, bending or shape defects.

In section 4, we present the numerical method used to detect defects and some numerical simulations. To avoid the so called "inverse crime" in the numerical tests, we use two different codes. We use a finite element based solver with PML [5] to generate the data from a waveguide with defects. A modal decomposition based solver allows us to recover the inhomogeneities from the simulated data. Only the second code is used in the inversion procedure.

2 Forward and inverse source problem in a waveguide

In this section, we present the tools required to study the forward and inverse source problems in a waveguide. First, we recall some classical results about the forward source problem and the modal decomposition. These results can also be found in [7, 10]. Next, we study the perturbed forward source problem. Assuming that the perturbation is small enough, we show existence, uniqueness, and stability of a solution to the problem. This perturbed problem will prove very useful in the following. Finally, we present an inversion strategy using the measurements of the wave field on a section of the waveguide for full and partial frequency data.

2.1 Forward source problem in a perfect waveguide

We consider a 2D infinite perfect waveguide $\Omega = \mathbb{R}\times(0,1)$ in which waves can propagate at frequency $k > 0$ according to the homogeneous Helmholtz equation

$$\Delta u_k + k^2 u_k = 0. \tag{2}$$

We choose a Neumann condition on the boundary $\partial\Omega$, but this condition can be changed to a Dirichlet or a Robin condition without altering of our results. It is known that the homogeneous Neumann spectral problem for the negative Laplacian on $(0,1)$ has an infinite sequence of eigenvalues λ_n for $n \in \mathbb{N}$, and that it is possible to find eigenvectors φ_n that form an orthonormal basis of $\mathrm{L}^2(0,1)$. Precisely,

$$\lambda_n = n^2\pi^2, \qquad \varphi_n = \begin{cases} 1 & \text{if } n = 0, \\ y \mapsto \sqrt{2}\cos(n\pi y) & \text{otherwise.} \end{cases} \tag{3}$$

This basis is very important in the study of waveguides since every function $f \in \mathrm{L}^2_{\mathrm{loc}}(\Omega)$ can be decomposed in a sum of modes:

$$f(x,y) = \sum_{n\in\mathbb{N}} f_n(x)\varphi_n(y) \quad \text{f.a.e } (x,y)\in\Omega, \qquad f_n \in \mathrm{L}^2_{\mathrm{loc}}(\mathbb{R}). \tag{4}$$

Let ν be the outward unit normal on $\partial\Omega$. Using this orthonormal basis, the solutions to the homogeneous problem

$$\begin{cases} \Delta u_k + k^2 u_k = 0 & \text{in } \Omega, \\ \partial_\nu u_k = 0 & \text{on } \partial\Omega, \end{cases} \tag{5}$$

are linear combinations of $(x,y) \mapsto \varphi_n(y)e^{\pm ik_n x}$ where $k_n^2 = k^2 - n^2\pi^2$ and $\mathrm{Re}(k_n), \mathrm{Im}(k_n) \geq 0$. This solution is called the n-th mode. In the following, we assume that $k_n \neq 0$, meaning that we do not choose a wavelength $k = n\pi$ for $n \in \mathbb{N}$. Two types of modes appear: if $n < k/\pi$ then $k_n \in \mathbb{R}$ and the modes are called propagative. If $n > k/\pi$, then $k_n \in i\mathbb{R}$ and the modes are called evanescent, meaning that their amplitude decays exponentially fast at one hand of the waveguide. An extra condition is then needed to ensure the uniqueness of a solution to the Helmholtz problem (5).

Definition 1. A solution $u_k \in \mathrm{H}^2_{\mathrm{loc}}(\Omega)$ of (2) is outgoing if it satisfies the radiation conditions:

$$\left| \langle u_k(x,\cdot), \varphi_n\rangle'(x)\frac{x}{|x|} - ik_n\langle u_k(x,\cdot),\varphi_n\rangle \right| \underset{|x|\to+\infty}{\longrightarrow} 0 \quad \forall n \in \mathbb{N}. \tag{6}$$

Remark 2. This condition is an adaptation of the Sommerfeld condition used in free space to our problem. The articles [10, 7] are using an other radiation condition called Dirichlet to Neumann condition, which is equivalent to our radiation condition when s is compactly supported.

Using the previous conditions, we show the following proposition whose proof is given in the Appendix A.

Proposition 3. For every $s \in \mathrm{L}^1(\Omega) \cap \mathrm{L}^2_{\mathrm{loc}}(\Omega)$, the problem

$$\begin{cases} \Delta u_k + k^2 u_k = -s & \text{in } \Omega, \\ \partial_\nu u_k = 0 & \text{on } \partial\Omega, \\ u_k \text{ is outgoing,} \end{cases} \tag{7}$$

has a unique solution $u_k \in \mathrm{H}^2_{\mathrm{loc}}(\Omega)$, which decomposes as

$$u_k(x,y) = \sum_{n\in\mathbb{N}} u_{k,n}(x)\varphi_n(y) \quad \text{where} \quad u_{k,n}(x) = \frac{i}{2k_n}\int_{\mathbb{R}} s_n(z)e^{ik_n|x-z|}\mathrm{d}z, \tag{8}$$

if the decomposition of s is $s(x,y) = \sum_{n\in\mathbb{N}} s_n(x)\varphi_n(y)$.

Remark 4. It is interesting to note that s does not need to have a compact support in this context, which is the case in the free space Helmholtz problem.

If we consider a restriction of the waveguide $\Omega_r := (-r,r)\times(0,1)$ where $r > 0$, we assume that every source defined on Ω_r is extented by 0 in Ω and we define the forward Helmholtz source operator $\mathcal{H}_k$ by

$$\mathcal{H}_k : \begin{array}{ccc} \mathrm{L}^2(\Omega_r) & \to & \mathrm{H}^2(\Omega_r) \\ s & \mapsto & u_{k\,|\Omega_r} \end{array} \qquad \text{where } u_k \text{ is solution to (7).} \tag{9}$$

The following proposition quantifies the dependence between u and the source s. Its proof is given in Appendix B.

Proposition 5. The forward Helmholtz source operator $\mathcal{H}_k$ is well defined, continuous and there exists $C > 0$ depending only on k and r such that for every $s \in \mathrm{L}^2(\Omega_r)$,

$$\|u_k\|_{\mathrm{H}^2(\Omega_r)} \leq C\|s\|_{\mathrm{L}^2(\Omega_r)}. \tag{10}$$

Remark 6. We notice in the proof that C increases when the distance between k and $\pi\mathbb{N}$ decreases.

In the following, we also need to consider the problem where the source is located on the boundary of the waveguide. Let $\partial\Omega_{\mathrm{top}} = \mathbb{R} \times \{1\}$ and $\partial\Omega_{\mathrm{bot}} = \mathbb{R} \times \{0\}$. Similarly to Proposition 3, we have

Proposition 7. Let $b_1, b_2 \in \mathrm{L}^1(\mathbb{R}) \cap \mathrm{H}^{1/2}_{\mathrm{loc}}(\mathbb{R})$. The problem

$$\begin{cases} \Delta u_k + k^2 u_k = 0 & \text{in } \Omega, \\ \partial_\nu u_k = b_1 & \text{on } \partial\Omega_{\mathrm{top}}, \\ \partial_\nu u_k = b_2 & \text{on } \partial\Omega_{\mathrm{bot}}, \\ u_k \text{ is outgoing}, \end{cases} \tag{11}$$

has a unique solution $u_k \in \mathrm{H}^2_{\mathrm{loc}}(\Omega)$, which decomposes as

$$u_k(x,y) = \sum_{n\in\mathbb{N}} u_{k,n}(x)\varphi_n(y) \text{ where } u_{k,n}(x) = \frac{i}{2k_n}\int_{\mathbb{R}} (b_1(z)\varphi_n(1) + b_2(z)\varphi_n(0))e^{ik_n|x-z|}\mathrm{d}z. \tag{12}$$

In the restricted guide Ω_r, we assume again that every source defined on $(-r, r)$ is extended by 0 on $\mathbb{R}$ and we define the forward Helmholtz boundary source operator $\mathcal{G}_k$ by

$$\begin{array}{rccll} \mathcal{G}_k : & \left(\widetilde{\mathrm{H}}^{1/2}(-r,r)\right)^2 & \to & \mathrm{H}^2(\Omega_r) & \text{where } u_k \text{ is the solution to (11),} \\ & (b_1, b_2) & \mapsto & u_k & \end{array} \tag{13}$$

and $\widetilde{\mathrm{H}}^{1/2}(-r,r)$ is the closure of $\mathcal{D}(-r,r)$, the distribution on $(-r,r)$, in $\mathrm{H}^{1/2}(\mathbb{R})$ (see [17] for more details). A result similar to Proposition 5 holds:

Proposition 8. The forward Helmholtz boundary source operator $\mathcal{G}_k$ is well defined, continuous and there exists a constant D depending only on k and r such that for every $b_1, b_2 \in \widetilde{\mathrm{H}}^{1/2}(-r,r)$,

$$\|\mathcal{G}(b_1,b_2)\|_{\mathrm{H}^2(\Omega_r)} \leq D\left(\|b_1\|_{\widetilde{\mathrm{H}}^{1/2}{}_{(-r,r)}} + \|b_2\|_{\widetilde{\mathrm{H}}^{1/2}{}_{(-r,r)}}\right). \tag{14}$$

Remark 9. Combining Proposition 3 and 7, we see by linearity that the problem

$$\begin{cases} \Delta u_k + k^2 u_k = -s & \text{in } \Omega, \\ \partial_\nu u_k = b_1 & \text{on } \partial\Omega_{\mathrm{top}}, \\ \partial_\nu u_k = b_2 & \text{on } \partial\Omega_{\mathrm{bot}}, \\ u_k \text{ is outgoing}, \end{cases} \tag{15}$$

has a unique solution $u_k \in \mathrm{H}^2_{\mathrm{loc}}(\Omega)$.

2.2 Forward source problem with perturbations

In the following we introduce a theoretical framework for a perturbed Helmholtz problem in a perfect waveguide. Under the Born hypothesis, we prove existence and uniqueness of a solution for the perturbed problem. Then, we provide a control of the error between the exact solution for the perturbed problem and its Born approximation.

Let us consider the following perturbed Helmholtz problem

$$\begin{cases} \Delta w_k + k^2 w_k = -s - f(w_k) & \text{in } \Omega, \\ \partial_\nu w_k = b_1 + g_1(w_k) & \text{on } \partial\Omega_{\text{top}}, \\ \partial_\nu w_k = b_2 + g_2(w_k) & \text{on } \partial\Omega_{\text{bot}}, \\ w_k \text{ is outgoing}, \end{cases} \tag{16}$$

where f, g_1, g_2 are linear functions depending on w_k. Moreover, we assume that there exists $r > 0$ such that $\text{supp}(f(w_k)) \subset \Omega_r$ and $\text{supp}(g_1(w_k)), \text{supp}(g_2(w_k)) \subset (-r, r)$ for every $w_k \in \mathrm{H}^2_{\text{loc}}(\Omega)$.

Using the forward Helmholtz source operator $\mathcal{H}_k$ and the forward Helmholtz boundary source operator $\mathcal{G}_k$ defined in (9) and (13), we can rewrite this equation on Ω_r:

$$w_k = \mathcal{H}_k(s) + \mathcal{G}_k(b_1, b_2) + \mathcal{H}_k(f(w_k)) + \mathcal{G}_k(g_1(w_k), g_2(w_k)). \tag{17}$$

Proposition 10. Let $r > 0$ such that $f \in \mathcal{L}_c\left(\mathrm{H}^2(\Omega_r), \mathrm{L}^2(\Omega_r)\right)$ and $g_1, g_2 \in \mathcal{L}_c\left(\mathrm{H}^2(\Omega_r), \widetilde{\mathrm{H}}^{1/2}(-r, r)\right)$ where $\mathcal{L}_c$ denote the linear continuous applications. Let C and D be the constants defined in Propositions 5 and 8. Let $s \in \mathrm{L}^2(\Omega_r)$, $b_1, b_2 \in \widetilde{\mathrm{H}}^{1/2}(-r, r)$ and assume that

$$\mu := C\|f\|_{\mathcal{L}_c\left(\mathrm{H}^2(\Omega_r), \mathrm{L}^2(\Omega_r)\right)} + D\left(\|g_1\|_{\mathcal{L}_c\left(\mathrm{H}^2(\Omega_r), \widetilde{\mathrm{H}}^{1/2}(-r,r)\right)} + \|g_2\|_{\mathcal{L}_c\left(\mathrm{H}^2(\Omega_r), \widetilde{\mathrm{H}}^{1/2}(-r,r)\right)}\right) < 1. \tag{18}$$

Then (17) has a unique solution $w_k \in \mathrm{H}^2(\Omega_r)$ and

$$w_k = \sum_{m \in \mathbb{N}} \left[\mathcal{H}_k \circ f + \mathcal{G}_k \circ (g_1, g_2)\right]^m \left(\mathcal{H}_k(s) + \mathcal{G}_k(b_1, b_2)\right). \tag{19}$$

Proof. If (18) is satisfied then $\mathcal{H}_k \circ f + \mathcal{G}_k \circ (g_1, g_2)$ is a contraction, and the expression (19) is the expansion of w_k into a Born series (see for instance [9]). □

To compute numerically w_k, we approximate the Born series by its first term.

Definition 11. Let w_k be defined by (19). We define v_k, the Born approximation of w_k by

$$v_k = \mathcal{H}_k(s) + \mathcal{G}_k(b_1, b_2). \tag{20}$$

Proposition 12. Using the assumption (18) on μ as in Proposition 10, let w_k be the solution of (17) and v_k its Born approximation. Then

$$\|w_k - v_k\|_{\mathrm{H}^2(\Omega_r)} \leq \left(C\|s\|_{\mathrm{L}^2(\Omega_r)} + D\left(\|b_1\|_{\widetilde{\mathrm{H}}^{1/2}(-r,r)} + \|b_2\|_{\widetilde{\mathrm{H}}^{1/2}(-r,r)}\right)\right) \frac{\mu}{1-\mu} \tag{21}$$

Proof. We use the definition of w_k and v_k and the sum of geometrical series. □

Remark 13. If f, g_1 and g_2 are small, we have proved that the solution of (16) is very close to the solution of

$$\begin{cases} \Delta v_k + k^2 v_k = -s & \text{in } \Omega, \\ \partial_\nu v_k = b_1 & \text{on } \partial\Omega_{\text{top}}, \\ \partial_\nu v_k = b_2 & \text{on } \partial\Omega_{\text{bot}}, \\ v_k \text{ is outgoing}, \end{cases} \tag{22}$$

and we have quantified the error made by approximating w_k by v_k.

2.3 Inverse source problem in a perfect waveguide

We go back to Problem (7) with a real-valued source s and we assume that measurements are made on the section $\{0\} \times (0,1)$ for every frequency $k > 0$. Using this measurements, we try and determine the location of the source s.

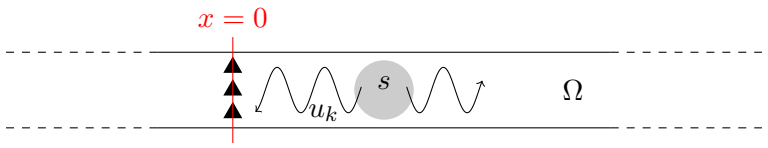

For every $k > 0$, we measure $u_k(0, y)$ for every $y \in (0,1)$. Using Proposition 3, we know that

$$u_k(0,y) = \sum_{n\in\mathbb{N}} u_{k,n}(0)\varphi_n(y) \quad \text{where} \quad u_{k,n}(0) = \frac{i}{2k_n}\int_{\mathbb{R}} s_n(z)e^{ik_n|z|}\mathrm{d}z, \tag{23}$$

if the decomposition of s is $s(x,y) = \sum_{n\in\mathbb{N}} s_n(x)\varphi_n(y)$. Since $u_{k,n}(0) = \int_{\mathbb{R}} u_k(0,y)\varphi_n(y)\mathrm{d}y$, we can theoretically have acces to $u_{k,n}(0)$ for every $n \in \mathbb{N}$. However, to be closer to the experiments, we assume that we can only measure the propagative modes, meaning that we have access to $u_{k,n}(0)$ for every $n \in \mathbb{N}$ such that $n < k/\pi$:

$$u_{k,n}(0) = \frac{i}{2k_n}\int_{\mathbb{R}} s_n(z)e^{ik_n|z|}\mathrm{d}z \quad \forall k > 0,\ \forall n \in \mathbb{N},\ n < k/\pi. \tag{24}$$

We notice that this expression depends on $k_n = \sqrt{k^2 - n^2\pi^2}$. Since $(k,n) \mapsto (\sqrt{k^2 - n^2\pi^2}, n)$ is one-to-one from $\{(k,n) \in \mathbb{R}_+^* \times \mathbb{N},\ n < k/\pi\}$ to $\mathbb{R}_+^* \times \mathbb{N}$, the available data is then

$$d_{\omega,n} := \frac{i}{2\omega}\int_{\mathbb{R}} s_n(z)e^{i\omega|z|}\mathrm{d}z \quad \forall n \in \mathbb{N},\ \forall \omega \in \mathbb{R}_+^*. \tag{25}$$

This change of variable means that given a mode n and a value $\omega > 0$, there exists a frequency $k > 0$ such that n is a propagative mode and $k_n = \omega$. In order to remove the absolute value in the expression of the available data, we assume that $\mathrm{supp}(s) \subset (0, +\infty) \times (0,1)$, which means that the source is located to the right of the section where the measurements are made.

Definition 14. Let H be the Hilbert space defined by

$$\mathrm{H} := \left\{ \hat{u} : \mathbb{R}_+^* \to \mathbb{C} \quad | \quad \int_0^{+\infty} \omega^2 |\hat{u}(\omega)|^2 \mathrm{d}\omega < +\infty \right\}, \qquad \|\hat{u}\|_{\mathrm{H}}^2 = \int_0^{+\infty} \omega^2 |\hat{u}(\omega)|^2 \mathrm{d}k. \tag{26}$$

We denote by Γ the forward modal operator and by F_{source} the forward source operator for problem (7). Then Γ and F_{source} are defined by

$$\Gamma : \begin{array}{ccc} \mathrm{L}^2(\mathbb{R}_+) & \to & \mathrm{H} \\ f & \mapsto & \left(\omega \mapsto \dfrac{i}{2\omega}\displaystyle\int_0^{+\infty} f(z)e^{i\omega z}\mathrm{d}z\right) \end{array}, \qquad F_{\text{source}} : \begin{array}{ccc} \mathrm{L}^2(\Omega) & \to & \ell^2(\mathrm{H}) \\ s & \mapsto & (\Gamma(s_n))_{n\in\mathbb{N}} \end{array}, \tag{27}$$

if the decomposition of s is $s(x,y) = \displaystyle\sum_{n\in\mathbb{N}} s_n(x)\varphi_n(y)$.

We choose the following definition for the Fourier transform:

$$\mathcal{F}(f)(\omega) = \int_{\mathbb{R}} f(z)e^{-i\omega z}\mathrm{d}z.$$

Since s is real-valued, Γ is related to the Fourier transform:

$$\mathcal{F}(f)(\omega) = \begin{cases} \overline{\frac{2\omega}{i}\Gamma(f)(\omega)} & \text{if } \omega > 0 \\ \frac{-2\omega}{i}\Gamma(f)(-\omega) & \text{if } \omega < 0 \end{cases}.$$

Using the properties of the Fourier transform, we can prove the following Proposition:

Proposition 15. The forward modal operator Γ and the forward source operator F_{source} satisfy the relations

$$\|\Gamma(f)\|_{\mathrm{H}}^2 = \frac{\pi}{4}\|f\|_{\mathrm{L}^2(\mathbb{R}_+)}^2 \quad \forall f \in \mathrm{L}^2(\mathbb{R}_+), \qquad \|F_{\text{source}}(s)\|_{\mathrm{l}^2(\mathrm{H})}^2 = \frac{\pi}{4}\|s\|_{\mathrm{L}^2(\Omega)}^2 \quad \forall s \in \mathrm{L}^2(\Omega), \tag{28}$$

and their inverse operators are given by

$$\Gamma^{-1} : \begin{array}{ccc} \mathrm{H} & \to & \mathrm{L}^2(\mathbb{R}) \\ v & \mapsto & \left(x \mapsto \dfrac{1}{2\pi}\displaystyle\int_0^{+\infty} \frac{-2\omega}{i}\overline{v(\omega)}e^{i\omega x}\mathrm{d}\omega + \frac{1}{2\pi}\int_{-\infty}^{0} \frac{-2\omega}{i}v(-\omega)e^{i\omega x}\mathrm{d}\omega\right) \end{array}, \tag{29}$$

$$F_{\text{source}}^{-1} : \begin{array}{ccc} \ell^2(\mathrm{H}) & \to & \mathrm{L}^2(\Omega) \\ (v_n)_{n\in\mathbb{N}} & \mapsto & \left((x,y) \mapsto \displaystyle\sum_{n\in\mathbb{N}} \Gamma^{-1}(v_n)(x)\varphi_n(y)\right) \end{array}. \tag{30}$$

We can use the same framework for problem (11). Using the fact that

$$u_{k,n}(0) = \frac{i}{2k_n}\int_{\mathbb{R}}(-b_1(z)\varphi_n(1) + b_2(z)\varphi_n(0))e^{ik_n|z|}\mathrm{d}z \quad \forall n \in \mathbb{N}, \tag{31}$$

and that $(k,n) \mapsto (\sqrt{k^2 - n^2\pi^2}, n)$ is one-to-one from $\{(k,n) \in \mathbb{R}_+^* \times \mathbb{N},\ n < k/\pi\}$ to $\mathbb{R}_+^* \times \mathbb{N}$, the available data is

$$d_{\omega,1} = \frac{i}{2\omega}\int_{\mathbb{R}}(b_1(z)+b_2(z))e^{i\omega|z|}\mathrm{d}z, \quad d_{\omega,2} = \frac{i}{2\omega}\int_{\mathbb{R}}(-\sqrt{2}b_1(z)+\sqrt{2}b_2(z))e^{i\omega|z|}\mathrm{d}z \qquad \forall \omega \in \mathbb{R}_+^*. \tag{32}$$

Again, we assume that $\mathrm{supp}(b_1), \mathrm{supp}(b_2) \subset (0, +\infty)$ and we define the forward operator.

Definition 16. We denote F_{bound} the forward Helmholtz boundary source operator for the problem (11), defined by

$$F_{\text{bound}} : \begin{array}{ccc} \left(\mathrm{H}^{1/2}(\mathbb{R}_+)\right)^2 & \to & \mathrm{H}\times\mathrm{H} \\ (b_1,b_2) & \mapsto & \begin{pmatrix} \omega \mapsto \dfrac{i}{2\omega}\displaystyle\int_0^{+\infty}(b_1(z)+b_2(z))e^{i\omega z}\mathrm{d}z \\ \omega \mapsto \dfrac{i}{\sqrt{2}\omega}\displaystyle\int_0^{+\infty}(-b_1(z)+b_2(z))e^{i\omega z}\mathrm{d}z \end{pmatrix} \end{array}. \tag{33}$$

Remark 17. This operator is well defined according to Proposition 7.

We notice that we only need the first two modes $n=0$ and $n=1$ to identify b_1 and b_2:

Proposition 18. The forward Helmholtz boundary source operator F_{bound} is invertible:

$$F_{\text{bound}}^{-1} : \begin{array}{ccc} \mathrm{H}\times\mathrm{H} & \to & \left(\mathrm{H}^{1/2}(\mathbb{R}_+)\right)^2 \\ (v_1,v_2) & \mapsto & \left(\Gamma^{-1}\left(\dfrac{\sqrt{2}v_1-v_2}{2\sqrt{2}}\right),\Gamma^{-1}\left(\dfrac{\sqrt{2}v_1+v_2}{2\sqrt{2}}\right)\right) \end{array}. \tag{34}$$

Propositions 15 and 18 show that the measurements of the wave on a section of the waveguide at all frequencies are sufficient to reconstruct the source. Thus, inverse operators can be computed explicitly and in a stable way. However, the assumption of knowing u_k for every $k>0$ is unrealistic in practice. We address this issue of limited data in the next subsection.

2.4 Inverse source problem from limited frequency data

In this section, we assume that the frequency data are only known in a given interval. To reconstruct every s_n in (7), we need to find a way to reconstruct a function f knowing only the values of its Fourier transform on a given interval. If this given interval is in the form $(0,\omega_1)$, some regularity on the function is enough to provide a good reconstruction of f and a control on the error of approximation (see for instance [12]). On the other hand, we have to deal in the next section with intervals of the form $(\omega_0,+\infty)$. This case is harder, and it seems difficult to get a good reconstruction of the function f. However, if the function f is compactly supported, its Fourier transform is analytic. Thus, the values of $\Gamma(f)(\omega)$ for ω in a interval (ω_0,ω_1) completely determine $\Gamma(f)(\omega)$ for ω in $(0,+\infty)$. In the following, we address the issue of the stability of this reconstruction.

We start with a lemma to control the L^2 norm on $(0,\omega_0)$ of an analytic function given its norm on $(\omega_0,\omega_0+\sigma)$ where ω_0 and σ are positive real numbers.

Lemma 19. Let f be a function in $\mathcal{C}^\infty(\mathbb{R}_+)\cap\mathrm{L}^2(\mathbb{R}_+)$ and assume that for every $j\in\mathbb{N}$ and $\omega\in\mathbb{R}_+$, $|f^{(j)}(\omega)|\leq c\frac{r^j}{j^\alpha}\|f\|_{L^2(\mathbb{R}_+)}$ where $r,\alpha,c\in\mathbb{R}_+^*$. Let $\omega_0,\sigma\in\mathbb{R}_+^*$ and $\varepsilon\in(0,1)$. There exists a constant ξ depending only on $\omega_0,\sigma,r,\alpha,c,\varepsilon$ such that

$$\frac{\|f\|_{\mathrm{L}^2(0,\omega_0)}}{\|f\|_{\mathrm{L}^2(\mathbb{R}^+)}}\leq\xi\left(\frac{\|f\|_{\mathrm{L}^2(\omega_0,\omega_0+\sigma)}}{\|f\|_{\mathrm{L}^2(\mathbb{R}^+)}}\right)^{1-\varepsilon}. \tag{35}$$

Proof. Let $n\in\mathbb{N}$, we define $\delta_j=c\frac{r^j}{j^\alpha}$ and write the Taylor expansion of f at ω_0 up to order n:

$$f(\omega)=\sum_{j=0}^{n}\frac{(\omega-\omega_0)^j}{j!}f^{(j)}(\omega_0)+R_n(\omega)\qquad\text{with}\qquad|R_n(\omega)|\leq\frac{\delta_{n+1}\|f\|_{L^2(\mathbb{R}_+)}|\omega-\omega_0|^{n+1}}{(n+1)!}.$$

We denote by $P_n \in \mathbb{R}_n[X]$ the Taylor polynomial associated with this expansion:

$$P_n = \sum_{j=0}^{n} a_j (X-\omega_0)^j := \sum_{j=0}^{n} \frac{f^{(j)}(\omega_0)}{j!}(X-\omega_0)^j,$$

and the operator

$$I_n : \begin{array}{ccc} \mathbb{R}_n[X] \cap \mathrm{L}^2(\omega_0, \omega_0+\sigma) & \to & \mathbb{R}_n[X] \cap \mathrm{L}^2(0,\omega_0) \\ P & \mapsto & P \end{array}.$$

endowed with the norm

$$\|I_n\| := \sup_{P \in \mathbb{R}_n[X]} \frac{\|P\|_{\mathrm{L}^2(0,\omega_0)}}{\|P\|_{\mathrm{L}^2(\omega_0,\omega_0+\sigma)}}.$$

We immediately see that

$$\begin{aligned} \|f\|_{\mathrm{L}^2(0,\omega_0)} &\leq \|f-P_n\|_{\mathrm{L}^2(0,\omega_0)} + \|P_n\|_{\mathrm{L}^2(0,\omega_0)} \\ &\leq \|R_n\|_{\mathrm{L}^2(0,\omega_0)} + \|I_n\|\|P_n\|_{\mathrm{L}^2(\omega_0,\omega_0+\sigma)} \\ &\leq \|R_n\|_{\mathrm{L}^2(0,\omega_0)} + \|I_n\|\|R_n\|_{\mathrm{L}^2(\omega_0,\omega_0+\sigma)} + \|I_n\|\|f\|_{\mathrm{L}^2(\omega_0,\omega_0+\sigma)}. \end{aligned} \tag{36}$$

Let us compute $\|I_n\|$. Let $P = \sum_{j=0}^n a_k (X-\omega_0)^j$ be a polynomial in $\mathbb{R}_n[X]$, then

$$\|P\|^2_{\mathrm{L}^2(0,\omega_0)} = \int_0^{\omega_0} \sum_{k,p=0}^{n} a_k a_p (\omega-\omega_0)^{k+p} \mathrm{d}\omega = \sum_{k,p=0}^{n} a_k a_p \frac{-(-\omega_0)^{k+p+1}}{k+p+1} = \omega_0 W^T H_n W,$$

where $W := \left(a_k(-\omega_0)^k\right)_{k=0,\cdots,n}$ and $H_n = \left(\frac{1}{k+p+1}\right)_{p,k=0,\cdots,n}$ is the Hilbert matrix. In the same way,

$$\|P\|^2_{\mathrm{L}^2(\omega_0,\omega_0+\sigma)} = \int_{\omega_0}^{\omega_0+\sigma} \sum_{k,p=0}^{n} a_k a_p (\omega-\omega_0)^{k+p} \mathrm{d}\omega = \sum_{k,p=0}^{n} a_k a_p \frac{\sigma^{k+p+1}}{k+p+1} = \sigma V^T H_n V.$$

where $V := \left(a_k \sigma^k\right)_{k=0,\cdots,n}$. Let $\lambda_{\min}$ and $\lambda_{\max}$ be the lowest and greatest eigenvalues of H_n. It follows that

$$\omega_0 W^T H_n W \leq \omega_0 \|W\|_2^2 \lambda_{\max}, \qquad \sigma V^T H_n V \geq \sigma \|V\|_2^2 \lambda_{\min}. \tag{37}$$

Notice that

$$\|W\|_2^2 \leq \max(1,\omega_0)^{2n} \sum_{k=0}^{n} |a_k|^2 \leq \frac{\max(1,\omega_0)^{2n}}{\min(1,\sigma)^{2n}} \sum_{k=0}^{n} |a_k|^2 \sigma^{2k} \leq \frac{\max(1,\omega_0)^{2n}}{\min(1,\sigma)^{2n}} \|V\|_2^2.$$

Thus, if $\omega_0 \leq \sigma$, then $\|W\|_2^2 \leq \|V\|_2^2$. We follow [18] to get an estimation of the condition number of the Hilbert matrix: There exists $c_H > 0$ such that $\mathrm{cond}_2(H_n)$ for the euclidean norm satisfies

$$\frac{\lambda_{\max}}{\lambda_{\min}} = \mathrm{cond}_2(H_n) \leq c_H \frac{(1+\sqrt{2})^{4n}}{\sqrt{n}}.$$

We conclude that

$$\|P\|^2_{\mathrm{L}^2(0,\omega_0)} \leq \frac{\omega_0}{\sigma} \left(1_{\omega_0 \leq \sigma} + 1_{\omega_0 > \sigma} \frac{\max(1,\omega_0)^{2n}}{\min(1,\sigma)^{2n}}\right) c_H \frac{(1+\sqrt{2})^{4n}}{\sqrt{n}} \|P\|^2_{\mathrm{L}^2(\omega_0,\omega_0+\sigma)}.$$

We define $c_1 := \sqrt{\frac{c_H \omega_0}{\sigma}}$ and $c_2 := \left(1+\sqrt{2}\right)^2 \left(1_{\omega_0 \leq \sigma} + 1_{\omega_0 > \sigma} \frac{\max(1,\omega_0)}{\min(1,\sigma)}\right)$, then

$$\|I_n\| \leq c_1 \frac{c_2^n}{n^{1/4}}. \tag{38}$$

We next bound R_n in $\mathrm{L}^2(0,\omega_0)$ by

$$\|R_n\|_{\mathrm{L}^2(0,\omega_0)} \leq \frac{\delta_{n+1}\|f\|_{\mathrm{L}^2(\mathbb{R}_+)}}{(n+1)!}\left(\int_0^{\omega_0}(\omega_0-\omega)^{2n+2}\mathrm{d}\omega\right)^{1/2} = \frac{\delta_{n+1}\|f\|_{\mathrm{L}^2(\mathbb{R}_+)}}{(n+1)!}\left(\frac{\omega_0^{2n+3}}{2n+3}\right)^{1/2},$$

and in $\mathrm{L}^2(\omega_0,\omega_0+\sigma)$ by

$$\|R_n\|_{\mathrm{L}^2(\omega_0,\omega_0+\sigma)} \leq \frac{\delta_{n+1}\|f\|_{\mathrm{L}^2(\mathbb{R}_+)}}{(n+1)!}\left(\int_{\omega_0}^{\omega_0+\sigma}(\omega-\omega_0)^{2n+2}\mathrm{d}\omega\right)^{1/2} = \frac{\delta_{n+1}\|f\|_{\mathrm{L}^2(\mathbb{R}_+)}}{(n+1)!}\left(\frac{\sigma^{2n+3}}{2n+3}\right)^{1/2}.$$

Substituting in (36) we find

$$\|f\|_{\mathrm{L}^2(0,\omega_0)} \leq \frac{\delta_{n+1}\|f\|_{\mathrm{L}^2(\mathbb{R}_+)}}{(n+1)!}\frac{\omega_0^{n+3/2}}{\sqrt{2n+3}} + \frac{\delta_{n+1}\|f\|_{\mathrm{L}^2(\mathbb{R}_+)}}{(n+1)!}\frac{\sigma^{n+3/2}}{\sqrt{2n+3}}\frac{c_1 c_2^n}{n^{1/4}} + \frac{c_1 c_2^n}{n^{1/4}}\|f\|_{\mathrm{L}^2(\omega_0,\omega_0+\sigma)}. \tag{39}$$

To simplify the notations, we define

$$c_3 := \frac{2}{\sqrt{2}}\max\left(\omega_0^{1/2}, c_1\sigma^{1/2}\right) = \max\left(1,\sqrt{c_H}\right)\sqrt{2\omega_0},$$

$$c_4 := \max(\omega_0, \sigma c_2) = \max\left[\omega_0, \left(1+\sqrt{2}\right)^2\left(1_{\omega_0\leq\sigma}\sigma + 1_{\omega_0>\sigma}\frac{\sigma\max(1,\omega_0)}{\min(1,\sigma)}\right)\right] = \sigma c_2.$$

The expression (39) can simplified and

$$\frac{\|f\|_{\mathrm{L}^2(0,\omega_0)}}{\|f\|_{\mathrm{L}^2(0,+\infty)}} \leq c_3\frac{\delta_{n+1}c_4^{n+1}}{(n+1)!\sqrt{n+1}} + c_1 c_2^n \frac{\|f\|_{\mathrm{L}^2(\omega_0,\omega_0+\sigma)}}{\|f\|_{\mathrm{L}^2(0,+\infty)}} \qquad \forall n \in \mathbb{N}.$$

The first term does not depend on f, and this expression shows that it is impossible to obtain a Lipschitz estimation. To optimize this estimate, we play on the degree n of the polynomials. Indeed, the first therm on the right hand side may be large for small values of n, while the second blows up when n is large. We set $Q := \|f\|_{\mathrm{L}^2(\omega_0,\omega_0+\sigma)}/\|f\|_{\mathrm{L}^2(\mathbb{R}^+)}$ and for $\varepsilon \in (0,1)$ we choose the integer

$$n = \left\lfloor -\frac{\varepsilon}{\ln(c_2)}\ln(Q) + \frac{\ln(c_5)}{\ln(c_2)}\right\rfloor,$$

where $c_5 > 0$ is a constant to be determined later, and $\lfloor\,\rfloor$ is the floor function. As the Stirling formula shows that $n! \geq \sqrt{2\pi n}\frac{n^n}{e^n}$ and $\delta_{n+1} = c\frac{r^{n+1}}{(n+1)^\alpha}$,

$$c_3\frac{\delta_{n+1}c_4^{n+1}}{(n+1)!\sqrt{n+1}} \leq \frac{c_3 c(erc_4)^{n+1}}{(n+1)^{\alpha+1}\sqrt{2\pi}(n+1)^{n+1}} = \frac{c_3 c}{\sqrt{2\pi}}\frac{(erc_4)^{n+1}}{(n+1)^{n+\alpha+2}}.$$

To simplify the notations, we define

$$\gamma := erc_4, \quad A := \frac{\ln(c_5)}{\ln(c_2)}, \quad B := \frac{\varepsilon}{\ln(c_2)}.$$

Using the fact that $A - B\ln(Q) \leq n+1 \leq A - B\ln(Q)+1$, we see that

$$\begin{aligned}\frac{(ert)^{n+1}}{(n+1)^{n+\alpha+2}} &\leq \exp\left[(A-B\ln(Q)+1)\ln(\gamma) - (A-B\ln(Q)+\alpha+1)\ln(A-B\ln(Q))\right] \\ &= \gamma^{A+1}Q^{-B\ln(\gamma)+B\ln(A-B\ln(Q))}(A-B\ln(Q))^{-(A+\alpha+1)}.\end{aligned}$$

We want the power of Q to be greater that $1-\varepsilon$, and it is satisfied if

$$Q \leq \exp\left(-\frac{1}{B}\left[\exp\left(\frac{1-\varepsilon}{B}+\ln(\gamma)\right) - A\right]\right).$$

Since $Q \leq 1$, this condition is satisfied if

$$A = \exp\left(\frac{1-\varepsilon}{B}+\ln(\gamma)\right) + B\ln(\eta) = erc_4 c_2^{\frac{1-\varepsilon}{\varepsilon}} \quad \Leftrightarrow \quad c_5 = c_2^{erc_4 c_2^{\frac{1-\varepsilon}{\varepsilon}}}.$$

Using the fact that $A - B\ln(Q) \geq erc_4 c_2^{\frac{1-\varepsilon}{\varepsilon}}$, it follows that

$$\frac{\|f\|_{\mathrm{L}^2(0,\omega_0)}}{\|f\|_{\mathrm{L}^2(\mathbb{R}^+)}} \leq \xi\left(\frac{\|f\|_{\mathrm{L}^2(\omega_0,\omega_0+\sigma)}}{\|f\|_{\mathrm{L}^2(\mathbb{R}^+)}}\right)^{1-\varepsilon},$$

where

$$\xi := \frac{c_3 c}{\sqrt{2\pi}} c_2^{-\frac{1-\varepsilon}{\varepsilon}\left(1+\alpha+erc_4 c_2^{\frac{1-\varepsilon}{\varepsilon}}\right)} (erc_4)^{-\alpha} + c_1 c_2^{erc_4 c_2^{\frac{1-\varepsilon}{\varepsilon}}}. \tag{40}$$

□

Remark 20. The expression of ξ is not sharp most of the time, especially at step (37), which may over estimate the constant ξ.

We now consider two functions f and f_{app} of one variable. The following theorem provides a control over the distance between f and f_{app} using only the values of their Fourier transforms on the interval $[\omega_0, +\infty)$.

Theorem 21 (Reconstruction with low frequency gap in the Fourier transform)**.** Let $f, f_{\mathrm{app}} \in \mathrm{L}^2(-r,r)$ where $r \in \mathbb{R}_+^*$. Let $\omega_0, \sigma \in \mathbb{R}_+^*$. We assume that there exists $M \in \mathbb{R}_+^*$ such that

$$\|f\|_{\mathrm{L}^2(-r,r)} \leq M, \quad \|f_{\mathrm{app}}\|_{\mathrm{L}^2(-r,r)} \leq M. \tag{41}$$

For every $0 < \varepsilon < 1$, there exists ξ depending on $r, \omega_0, \sigma, \varepsilon$ such that

$$\|f - f_{\mathrm{app}}\|^2_{\mathrm{L}^2(-r,r)} \leq \frac{(8\pi M^2)^{\varepsilon}}{\pi}\xi^2 \|\mathcal{F}(f) - \mathcal{F}(f_{\mathrm{app}})\|^{2-2\varepsilon}_{\mathrm{L}^2(\omega_0,\omega_0+\sigma)} + \frac{1}{\pi}\|\mathcal{F}(f) - \mathcal{F}(f_{\mathrm{app}})\|^2_{\mathrm{L}^2(\omega_0,+\infty)}. \tag{42}$$

Proof. We know that

$$\|f - f_{\mathrm{app}}\|^2_{\mathrm{L}^2(-r,r)} = \frac{1}{\pi}\|\mathcal{F}(f) - \mathcal{F}(f_{\mathrm{app}})\|^2_{\mathrm{L}^2(0,\omega_0)} + \frac{1}{\pi}\|\mathcal{F}(f) - \mathcal{F}(f_{\mathrm{app}})\|^2_{\mathrm{L}^2(\omega_0,+\infty)}.$$

Since f is compactly supported as a function of $\mathrm{L}^2(\mathbb{R})$, we know that for every $j \in \mathbb{N}$, $\omega \in \mathbb{R}_+$,

$$\left|\frac{\mathrm{d}^j}{\mathrm{d}\omega^j}(\mathcal{F}(f) - \mathcal{F}(f_{\mathrm{app}}))(\omega)\right| \leq \left(2\int_0^r x^{2j}\mathrm{d}x\right)^{1/2} \|f - f_{\mathrm{app}}\|_{L^2(-r,r)} = \frac{r^j\sqrt{r}\|\mathcal{F}(f) - \mathcal{F}(f_{\mathrm{app}})\|_{L^2(\mathbb{R}_+)}}{\sqrt{\pi}\sqrt{2j+1}}.$$

It follows from Lemma 19 that

$$\|f - f_{\text{app}}\|^2_{\mathrm{L}^2(-r,r)} \leq \frac{1}{\pi}\xi^2 \|\mathcal{F}(f) - \mathcal{F}(f_{\text{app}})\|^{2\varepsilon}_{\mathrm{L}^2(\mathbb{R}^+)} \|\mathcal{F}(f) - \mathcal{F}(f_{\text{app}})\|^{2-2\varepsilon}_{\mathrm{L}^2(\omega_0,\omega_0+\sigma)} + \frac{1}{\pi}\|\mathcal{F}(f) - \mathcal{F}(f_{\text{app}})\|^2_{\mathrm{L}^2(\omega_0,+\infty)}.$$

Since $\|\mathcal{F}(f) - \mathcal{F}(f_{\text{app}})\|^{2\varepsilon}_{\mathrm{L}^2(\mathbb{R}^+)} \leq \left(2\pi\|f - f_{\text{app}}\|^2_{\mathrm{L}^2(-r,r)}\right)^{\varepsilon} \leq (8\pi M^2)^{\varepsilon}$, the result follows. □

Next, we generalize Theorem 21 to the case when we control the Fourier transform of f on a finite interval $[\omega_0, \omega_1]$.

Theorem 22 (Reconstruction with an interval of the Fourier transform)**.** Let $f, f_{\text{app}} \in \mathrm{H}^1(-r,r)$ where $r > 0$. Let $\omega_0, \omega_1 \in \mathbb{R}^*_+, \omega_0 < \omega_1$. We assume that there exists $M \in \mathbb{R}^*_+$ such that

$$\|f\|_{\mathrm{H}^1(-r,r)} \leq M, \quad \|f_{\text{app}}\|_{\mathrm{H}^1(-r,r)} \leq M. \tag{43}$$

For every $0 < \varepsilon < 1$, there exists ξ depending on $r, \omega_0, \omega_1, \varepsilon, M$ such that

$$\|f - f_{\text{app}}\|^2_{\mathrm{L}^2(-r,r)} \leq \frac{\left(8\pi M^2\right)^{\varepsilon}}{\pi}\xi^2 \|\mathcal{F}(f) - \mathcal{F}(f_{\text{app}})\|^{2-2\varepsilon}_{\mathrm{L}^2(\omega_0,\omega_1)} + \frac{1}{\pi}\|\mathcal{F}(f) - \mathcal{F}(f_{\text{app}})\|^2_{\mathrm{L}^2(\omega_0,\omega_1)} + \frac{8}{\omega_1^2}M^2. \tag{44}$$

Proof. We choose $\sigma = \max(1, \omega_1)$ in the Theorem 21. Since $f - f_{\text{app}} \in \mathrm{H}^1(-r,r)$,

$$\|\mathcal{F}(f) - \mathcal{F}(f_{\text{app}})\|^2_{\mathrm{L}^2(\omega_1,+\infty)} = \left\|\omega \mapsto \frac{\mathcal{F}(f')(\omega) - \mathcal{F}(f'_{\text{app}})(\omega)}{\omega}\right\|^2_{\mathrm{L}^2(\omega_1,+\infty)} \leq \frac{2\pi}{\omega_1^2}\|f' - f'_{\text{app}}\|^2_{\mathrm{L}^2(-r,r)}.$$

□

Remark 23. Using (40), we notice that $\xi \underset{\omega_0 \to 0}{\longrightarrow} 0$ and that $\frac{8\pi M^2}{\omega_1^2} \underset{\omega_1 \to +\infty}{\longrightarrow} 0$. Moreover, if we define $d = \Gamma(f)$ and $d_{\text{app}} = \Gamma(f_{\text{app}})$ then $2|\omega(d - d_{\text{app}})(\omega)| = |\mathcal{F}(f - f_{\text{app}})(\omega)|$ so

$$\frac{1}{\pi}\|\mathcal{F}(f) - \mathcal{F}(f_{\text{app}})\|^2_{\mathrm{L}^2(\omega_0,\omega_1)} \underset{[\omega_0,\omega_1]\to(0,+\infty)}{\longrightarrow} \frac{4}{\pi}\|d - \tilde{d}\|^2_{\mathrm{H}}, \tag{45}$$

and we recover the result of Proposition 15.

Theorem 22 provides a theoretical control of the error of the reconstruction between f and f_{app}. However, since ξ can be huge, such control might not be sufficient to ensure a numerical convergence of f_{app} to f. To illustrate this point, we consider a source s defined on X where X is the discretization of $[1-r, 1+r]$ with N_X points. We define $h = 2r/(N_X - 1)$. Using the fast Fourier transform, we compute the discretization of the Fourier transform $\mathcal{F}(s)$ on a set K of frequencies. We notice that $\mathcal{F}(s)(K) = Ms(X)$ where $M := h(e^{ixk})_{x\in X, k\in K}$, and that $s(X) = M^{-1}\mathcal{F}(s)(K)$. To simulate the low frequency gap, we define $K_t = \{k \in K, k > \omega_0\}$ and $M_t = h(e^{ixk})_{x\in X, k\in K_t}$. Then, $s(X) = M_t^{-1}\mathcal{F}(s)(K_t)$. Even if M_t is invertible, its condition number strongly depends on r and ω_0 just like the constant ξ in Lemma 19. Figure 2 illustrates this for different values of ω_0 and r. For a given value of condition number, only a few ω_0 allow a lower conditioning number if the source is small enough.

To conclude, if we only have access to perturbed Fourier transform data on a given interval of frequencies, we can build an approximation of f if f is compactly supported and if we know an *a priori* bound on the norm of f. However, depending of ω_0 and r, the error between f and the approximation of f can be very important. We can reduce it by increasing ω_1 and by diminishing ω_0 and r.

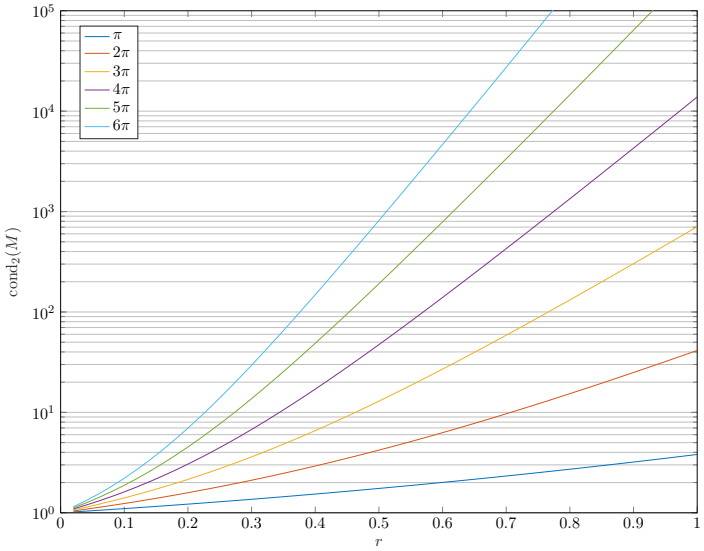

Figure 2: Condition number of M_t for different sizes of support and values of ω_0. Here, X is the discretization of $[1-r, 1+r]$ with $500r+1$ points. In the x-axis, we represent the evolution of r, and in the y-axis we represent $\mathrm{cond}_2(M_t)$. Each curve corresponds to a different value of ω_0 as indicated in the left rectangle.

3 Application to the identification of shape defects, bending or inhomogeneity

We propose a method to identify shape defects or bending of a waveguide, which is almost identical to that of source detection. We first map the deformed waveguide to a regular waveguide, and then use the inversion of source discussed in the first section to reconstruct the parameters that characterize the defect.

3.1 Mapping of the deformed waveguide

Let $\widetilde{\Omega}$ be a deformed waveguide. We assume that there exist ϕ_0 and ϕ_1 in $\mathcal{C}^1(\mathbb{R})$ such that

$$\widetilde{\Omega} = \bigcup_{x\in\mathbb{R}} (\phi_0(x), \phi_1(x)) = \{\phi_0(x) < y < \phi_1(x), x \in \mathbb{R}\}. \tag{46}$$

A wave $\tilde{u}$ in the deformed guide $\widetilde{\Omega}$ satisfies the equation

$$\begin{cases} \Delta\tilde{u} + k^2\tilde{u} = -\tilde{s} & \text{in } \widetilde{\Omega}, \\ \partial_\nu\tilde{u} = \tilde{b}_1 & \text{on } \partial\widetilde{\Omega}_{\mathrm{top}}, \\ \partial_\nu\tilde{u} = \tilde{b}_2 & \text{on } \partial\widetilde{\Omega}_{\mathrm{bot}}, \\ \tilde{u} \text{ is outgoing.} \end{cases} \tag{47}$$

where $\tilde{s} \in \mathrm{L}^2_{\mathrm{loc}}(\widetilde{\Omega})$, $\tilde{b_1} \in \mathrm{H}^{1/2}_{\mathrm{loc}}(\partial\widetilde{\Omega}_{\mathrm{top}})$, and $\tilde{b_2} \in \mathrm{H}^{1/2}_{\mathrm{loc}}(\partial\widetilde{\Omega}_{\mathrm{bot}})$. To use the tools developed in the previous section, we need to map $\widetilde{\Omega}$ to the regular waveguide $\Omega = (0,1)\times\mathbb{R}$. Let ϕ be a one-to-one function that maps Ω into $\widetilde{\Omega}$. Such a function exists and can even be assumed to be conformal (see

for instance [2]). We define $u = \tilde{u} \circ \phi$ the wave in the regular guide, and we try to find the equation satisfied by u. Let $J\phi$ be the Jacobien matrix of ϕ, $\tau = |\det(J\phi)|$, $t_1 = |\nabla \phi_0|$, and $t_2 = |\nabla \phi_1|$. The variational formulation of (47) shows that for every $\tilde{v} \in \mathrm{H}^1(\widetilde{\Omega})$,

$$\int_{\widetilde{\Omega}} \nabla \tilde{u} \cdot \nabla \tilde{v} - k^2 \int_{\widetilde{\Omega}} \tilde{u}\tilde{v} = \int_{\widetilde{\Omega}} \tilde{s}\tilde{v} + \int_{\partial\widetilde{\Omega}_{\mathrm{top}}} \tilde{b}_1 \tilde{v} + \int_{\partial\widetilde{\Omega}_{\mathrm{bot}}} \tilde{b}_2 \tilde{v}$$

$$\Leftrightarrow \int_{\Omega} \nabla \tilde{u} \circ \phi \cdot \nabla \tilde{v} \circ \phi \, \tau - k^2 \int_{\Omega} \tilde{u} \circ \phi \, \tilde{v} \circ \phi \, \tau = \int_{\Omega} \tilde{s} \circ \phi \, \tilde{v} \circ \phi \, \tau + \int_{\mathbb{R}} (\tilde{b}_1 \circ \phi_1 \, t_1 + \tilde{b}_2 \circ \phi_0 \, t_2) \, \tilde{v} \circ \phi. \quad (48)$$

Using the fact that $\nabla u = J\phi^T \nabla \tilde{u} \circ \phi$, we set $s = \tilde{s} \circ \phi$, $b_1 = \tilde{b}_1 \circ \phi_1$, $b_2 = \tilde{b}_2 \circ \phi_0$, and obtain that for every $v \in \mathrm{H}^1(\Omega)$,

$$\int_{\Omega} S\nabla u \cdot \nabla v - k^2 \int_{\Omega} u \, v \, \tau = \int_{\Omega} s \, v \, \tau + \int_{\partial\Omega_{\mathrm{top}}} b_1 \, v \, t_1 + \int_{\partial\Omega_{\mathrm{bot}}} b_2 \, v \, t_2. \quad (49)$$

where $S = J\phi^{-1} \left(J\phi^{-1}\right)^T \tau$, which yields the equation satisfied by u:

$$\begin{cases} \nabla \cdot (S\nabla u) + k^2 du = -\tau s & \text{in } \Omega, \\ S\nabla u \cdot \nu = b_1 t_1 & \text{on } \partial\Omega_{\mathrm{top}}, \\ S\nabla u \cdot \nu = b_2 t_2 & \text{on } \partial\Omega_{\mathrm{bot}}. \end{cases} \quad (50)$$

We can write $S = I_2 + M$ and $\tau = 1 + \varepsilon$, where M and ε are expected to be small if the deformation is small. The above partial differential equation becomes

$$\begin{cases} \Delta u + k^2 u = -\tau s - \nabla \cdot (M\nabla u) - k^2 \varepsilon u & \text{in } \Omega, \\ \nabla u \cdot \nu = b_1 t_1 - M\nabla u \cdot \nu & \text{on } \partial\Omega_{\mathrm{top}}, \\ \nabla u \cdot \nu = b_2 t_2 - M\nabla u \cdot \nu & \text{on } \partial\Omega_{\mathrm{bot}}. \end{cases} \quad (51)$$

We define two new operators for $r > 0$:

$$\Sigma : \begin{array}{ccc} \mathrm{H}^2(\Omega_r) & \to & \mathrm{L}^2(\Omega_r) \\ u & \mapsto & \nabla \cdot (M\nabla u) + k^2 \varepsilon u \end{array}, \qquad \Pi : \begin{array}{ccc} \mathrm{H}^2(\Omega_r) & \to & \widetilde{\mathrm{H}}^{1/2}(-r, r) \\ u & \mapsto & M\nabla u \cdot \nu \end{array}. \quad (52)$$

We use the definitions of Σ and Π and the dependence between $\|M\|_{\mathcal{C}^1(\Omega_r)}$, ε and ϕ to prove the following Proposition:

Proposition 24. The operator Σ and Π are continuous if $M \in \mathcal{C}^1(\Omega_r)$ and there exists constants $A(\phi), B(\phi)$ depending only on k and r such that

$$\|\Sigma(u)\|_{\mathrm{L}^2(\Omega_r)} \leq A(\phi)\|u\|_{\mathrm{H}^2(\Omega_r)}, \qquad \|\Pi(u)\|_{\mathrm{H}^{1/2}(\Omega_r)} \leq B(\phi)\|u\|_{\mathrm{H}^2(\Omega_r)}. \quad (53)$$

Using the results of Section 2.2 and Definition 11, we define the Born approximation v of u by

$$\begin{cases} \Delta v + k^2 v = -\tau s & \text{in } \Omega, \\ \nabla v \cdot \nu = b_1 t_1 & \text{on } \partial\Omega_{\mathrm{top}}, \\ \nabla v \cdot \nu = b_2 t_2 & \text{on } \partial\Omega_{\mathrm{bot}}, \\ v \text{ is outgoing.} \end{cases} \quad (54)$$

Proposition 10 and 12 yield the following:

Proposition 25. Let C and D be the constants defined in Propositions 5 and 8, and $A(\phi), B(\phi)$ defined in Proposition 24. If $CA(\phi) + 2DB(\phi) < 1$ then (51) has a unique solution u and

$$\|u - v\|_{\mathrm{H}^2(\Omega_r)} \leq \frac{CA(\phi) + 2DB(\phi)}{1 - CA(\phi) + 2DB(\phi)} \left(C\|\tau s\|_{\mathrm{L}^2(\Omega_r)} + D\left(\|b_2 t_2\|_{\widetilde{\mathrm{H}}^{1/2}{}_{(-r,r)}} + \|b_1 t_1\|_{\widetilde{\mathrm{H}}^{1/2}{}_{(-r,r)}} \right) \right). \tag{55}$$

Using the Born approximation, one is led to a problem similar to that of section 2. Using the results of inversion proved in this section, we are able to find τs, $b_1 t_1$ or $b_2 t_2$. In the following, we study how to characterize a defect by recovering one of those functions. For a bend, we can find an equation where $b_1 = b_2 = 0$, and we only need to find τs whereas for bumps, $s = 0$ and we need to find $b_1 t_1$ and $b_2 t_2$.

3.2 Detection of bends

We first consider the detection of a bend in the waveguide as depicted in Figure 3, which depends on three parameters: the distance x_c where the guide starts bending, the angle θ and the radius of curvature r.

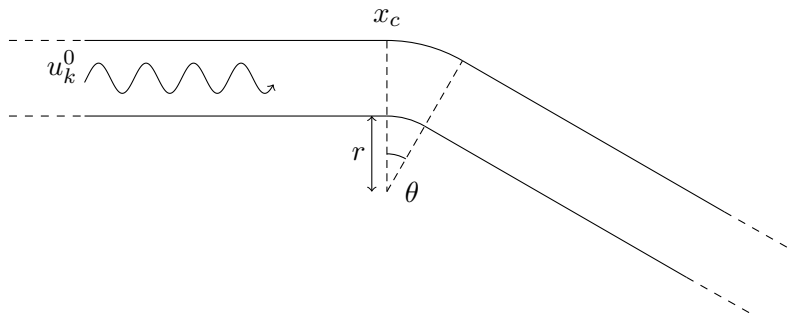

Figure 3: Representation of a bend in a waveguide.

More precisely, we define the mapping ϕ from Ω to $\widetilde{\Omega}$ as follow:

- If $x \leq x_c$, $\phi(x, y) = (x, y)$.
- If $x \in (x_c, x_c + \theta(r+1))$, then

$$\phi(x, y) = \left(x_c + (r + y) \sin\left(\frac{x - x_c}{r+1} \right), -r + (r + y) \cos\left(\frac{x - x_c}{r+1} \right) \right).$$

- If $x \geq x_c + \theta(r+1)$ then

$$\phi(x, y) = (x_c + (r+y)\sin\theta + (x - x_c - \theta(r+1))\cos\theta, -r + (r+y)\cos\theta - (x - x_c - \theta(r+1))\sin\theta).$$

Then we can see that $J\phi$ is an orthogonal matrix if $x \notin (x_c, x_c + \theta(r+1))$ and so $\tau = 1$. If $x \in (x_c, x_c + \theta(r+1))$, then

$$J\phi(x, y) = \begin{pmatrix} \frac{r+y}{r+1}\cos\left(\frac{x-x_c}{r+1}\right) & \sin\left(\frac{x-x_c}{r+1}\right) \\ -\frac{r+y}{r+1}\sin\left(\frac{x-x_c}{r+1}\right) & \cos\left(\frac{x-x_c}{r+1}\right) \end{pmatrix}, \quad \tau = \frac{r+y}{r+1},$$

$$S = J\phi^{-1}\left(J\phi^{-1}\right)^T \tau = \begin{pmatrix} \frac{r+1}{r+y} & 0 \\ 0 & \frac{r+y}{r+1} \end{pmatrix}. \tag{56}$$

Moreover, $t_1 = 1$ for every $x \in \mathbb{R}$, $t_2 = 1$ if $x \notin (x_c, x_c + \theta(r+1))$ and $t_2 = \frac{r}{r+1}$ otherwise.

We assume along this section that the bend is located to the right of the section $\{0\} \times (0,1)$. We introduce a source $\tilde{s}_k = -2ik\delta_0(x)$, and we notice that $s_k = \tilde{s}_k \circ \phi = \tilde{s}_k$. Without any defect, the wave field generated by this source would be $u_k^{\text{inc}} := e^{ik|x|}$. Let u_k^s be the scattered wave field defined by $u_k^s := u_k - u_k^{\text{inc}}$. Using (51), we notice that u_k^s satisfies the equation

$$\begin{cases} \nabla(S\nabla u_k^s) + k^2\tau u_k^s = -\tau s_k - \nabla(S\nabla u_k^{\text{inc}}) - k^2 d u_k^{\text{inc}} & \text{in } \Omega, \\ S\nabla u_k^s \cdot \nu = -S\nabla u_k^{\text{inc}} \cdot \nu & \text{on } \partial\Omega, \\ u_k^s \text{ is outgoing.} \end{cases} \tag{57}$$

The fact that $S\nabla u_k^{\text{inc}} \cdot \nu = 0$, and

$$-\tau s_k - \nabla(S\nabla u_k^{\text{inc}}) - k^2 d u_k^{\text{inc}} = -\mathbf{1}_{x\in[x_c,x_c+\theta(r+1)]} k^2 e^{ik|x|} h_r(y) = \mathbf{1}_{x\in[x_c,x_c+\theta(r+1)]} k^2 e^{ikx} h_r(y), \tag{58}$$

with $h_r(y) = (y-1)\left(\frac{1}{r+y} + \frac{1}{r+1}\right)$ leads to the equation

$$\begin{cases} \nabla(S\nabla u_k^s) + k^2\tau u_k^s = -\mathbf{1}_{x\in[x_c,x_c+\theta(r+1)]} k^2 e^{ikx} h_r(y) & \text{in } \Omega, \\ S\nabla u_k^s \cdot \nu = 0 & \text{on } \partial\Omega, \\ u_k^s \text{ is outgoing.} \end{cases} \tag{59}$$

If the assumptions of Proposition 25 are satisfied, u_k^s is close to the solution v_k of

$$\begin{cases} \Delta v_k + k^2 v_k = -\mathbf{1}_{x\in[x_c,x_c+\theta(r+1)]} k^2 e^{ikx} h_r(y) & \text{in } \Omega, \\ \nabla v_k \cdot \nu = 0 & \text{on } \partial\Omega, \\ v_k \text{ is outgoing.} \end{cases} \tag{60}$$

The measurements consist in the first mode $v_{k,0}$ of v_k for every frequency $k \in (0, k_{\max})$ where $k_{\max} \in \mathbb{R}_+^*$ is given. We define

$$f = \mathbf{1}_{x\in[x_c,x_c+\theta(r+1)]} \int_0^1 h_r(t)\mathrm{d}t. \tag{61}$$

Using Proposition 3 yields

$$v_{k,0}(0) = \frac{i}{2k}\int_0^{+\infty} k^2 f(y) e^{2iky}\mathrm{d}y = 2k^2\Gamma(f)(2k) \qquad \forall k \in (0, k_{\max}), \tag{62}$$

which shows that we have access to $\Gamma(f)(k)$ for all $k \in (0, 2k_{\max})$. We denote by $d = \Gamma(f)(k)$ the data and by d_{app} the perturbed data. We use the method described in section 2 to reconstruct f_{app} an approximation of f. The error of approximation is controlled by the following:

Proposition 26. Let f and f_{app} be two indicator functions supported in $(-a, a)$ where $a > 0$. We assume that the size of the supports of f and f_{app} is greater than δ. Let $k_{\max} \in R_+^*$, $d(k) = \Gamma(f)(k)$ and $d_{\text{app}}(k) = \Gamma(f_{\text{app}})(k)$ defined for $k \in (0, 2k_{\max})$. Let $c(k) = (\int_k^{+\infty} \operatorname{sinc}^2(x)\mathrm{d}x)^{1/2}$. Then there exists a constant $M \in \mathbb{R}_+^*$ such that

$$\|f - f_{\text{app}}\|^2_{\mathrm{L}^2(-a,a)} \leq \frac{4}{\pi}\|d - d_{\text{app}}\|^2_{\mathrm{H}} + Mc(\delta\, k_{\max}). \tag{63}$$

Proof. We notice that $|\mathcal{F}(f)(k)| = 2|k\Gamma(f)(k)|$ and we use the fact that the Fourier transform of a indicator function is of the form sinc. □

Remark 27. This bound of the error of approximation highlights two different sources of error: the error due to the perturbed data, and the error due to the lack of measurements for frequencies above $2k_{\max}$. The uncertainty of the measurements can lead to small perturbations of the data, but the most important source of perturbation is the Born approximation and the error given in Proposition 25.

To recover the parameters of the bend from f, we see that

$$\int_0^1 h_r(t)\mathrm{d}t = 1 - \frac{1}{2(r+1)} - (r+1)\ln\left(\frac{r+1}{r}\right) = -\frac{1}{r} + o_{r\to+\infty}\left(\frac{1}{r}\right).$$

If r is large enough, we can use the approximation $1/r$ or inverse the exact expression. Then, the support of f gives the values of x_c and θ.

To conclude, with the measurements on a section of the waveguide of the scattered field due to a source $\tilde{s}_k = -2ik\delta_0(x)$ for every frequency in $(0, k_{\max})$, we are able to reconstruct an approximation of f from which we can derive the parameters of the bend. Moreover, we can quantify the error of this approximation, and this error decreases as $k_{\max}$ increases and as θ decreases or r increases.

3.3 Detection of bumps

We now present a method to identify shape defects as those depicted in Figure 4 in the waveguide. Recovering a shape defect means finding the function h and g which describe the geometry of the waveguide.

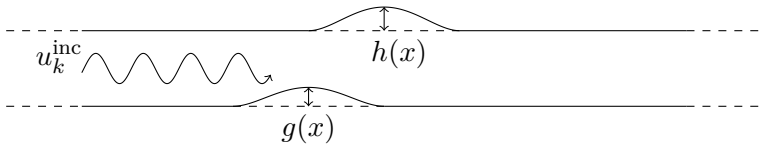

Figure 4: Representation of a shape defect in a waveguide.

We assume that $\mathrm{supp}(h), \mathrm{supp}(g)$ are compact, that $1 + h > g$, and that $h, g \in \mathcal{C}^2(\mathbb{R})$ so we can apply Proposition 25. We define $\phi(x, y) = (x, (1 + h(x) - g(x))y + g(x))$ and compute

$$J\phi(x,y) = \begin{pmatrix} 1 & 0 \\ (h'(x) - g'(x))y + g'(x) & 1 + h(x) - g(x) \end{pmatrix}, \tag{64}$$

$$J\phi^{-1}(x,y) = \begin{pmatrix} 1 & 0 \\ -\frac{(h'(x)-g'(x))y+g'(x)}{1+h(x)-g(x)} & \frac{1}{1+h(x)-g(x)} \end{pmatrix}.$$

Moreover, $\tau = |\det(J\phi)| = 1 + h(x) - g(x)$, $t_1 = \sqrt{1 + h'(x)^2}$, $t_2 = \sqrt{1 + g'(x)^2}$ and

$$S = J\phi^{-1}\left(J\phi^{-1}\right)^T\tau = \begin{pmatrix} 1 + h(x) - g(x) & -(h'(x) - g'(x))y - g'(x) \\ -(h'(x) - g'(x))y - g'(x) & \frac{((h'(x)-g'(x))y+g'(x))^2}{1+h(x)-g(x)} + \frac{1}{1+h(x)-g(x)} \end{pmatrix}.$$

We assume along this section that the bumps are located to the right of the section $\{0\} \times (0,1)$. We introduce a source $\tilde{s}_k = -2ik\delta_0(x)$, and we notice that $s_k = \tilde{s}_k \circ \phi = \tilde{s}_k$. Without any defect, the wave field generated by this source would be $u_k^{\text{inc}} := e^{ik|x|}$. Let $\tilde{u_k}^s$ be the scattered wave field defined by $\tilde{u_k^s} := \tilde{u_k} - u_k^{\text{inc}}$. We know that $\tilde{u_k}$ satisfies the equation

$$\begin{cases} \Delta \tilde{u_k} + k^2 \tilde{u_k} = \tilde{s}_k & \text{in } \widetilde{\Omega}, \\ \partial_\nu \tilde{u_k} = 0 & \text{on } \partial\widetilde{\Omega}, \\ \tilde{u_k} \text{ is outgoing.} \end{cases} \tag{65}$$

Using the expression of u_k^{inc} and the fact that if $x > 0$ then $e^{ik|x|} = e^{ikx}$, $\tilde{u_k}^s$ satisfies the equation

$$\begin{cases} \Delta \tilde{u_k}^s + k^2 \tilde{u_k}^s = 0 & \text{in } \widetilde{\Omega}, \\ \partial_\nu \tilde{u_k}^s = \frac{h'(x)}{\sqrt{1+h'(x)^2}} ike^{ikx} & \text{on } \partial\widetilde{\Omega}_{\text{top}}, \\ \partial_\nu \tilde{u_k}^s = \frac{-g'(x)}{\sqrt{1+g'(x)^2}} ike^{ikx} & \text{on } \partial\widetilde{\Omega}_{\text{bot}}, \\ \tilde{u_k}^s \text{ is outgoing.} \end{cases} \tag{66}$$

Using the transformation of a deformed guide to a regular guide and the equation (51), we obtain the problem satisfied in the regular guide Ω:

$$\begin{cases} \Delta u_k^s + k^2 u_s = -\nabla \cdot (M \nabla u_k^s) - k^2 \varepsilon u_k^s & \text{in } \Omega, \\ \partial_\nu u_k^s = -M \nabla u_k^s \cdot \nu + h'(x) ike^{ikx} & \text{on } \Omega_{\text{top}}, \\ \partial_\nu u_k^s = -M \nabla u_k^s \cdot \nu - g'(x) ike^{ikx} & \text{on } \Omega_{\text{bot}}, \\ u_k^s \text{ is outgoing.} \end{cases} \tag{67}$$

If the assumptions of Proposition 25 are satisfied, u_k^s is close to the solution v_k of

$$\begin{cases} \Delta v_k + k^2 v_k = 0 & \text{in } \Omega, \\ \partial_\nu v_k = h'(x) ike^{ikx} & \text{on } \Omega_{\text{top}}, \\ \partial_\nu v_k = -g'(x) ike^{ikx} & \text{on } \Omega_{\text{bot}}, \\ v_k \text{ is outgoing.} \end{cases} \tag{68}$$

Given $k_{\max} > 0$, we can measure the first mode $v_{k,0}$ of v_k for all frequencies $k \in (0, k_{\max})$. However, since we assumed that we can measure only propagative modes, we have access to $v_{k,1}$ the second mode of v_k for all frequencies $k > \pi$, so for $k \in (\pi, k_{\max})$. Using Proposition 7 and the inversion of source, we have access to

$$v_{k,0}(0) = \frac{i}{2k} \int_0^{+\infty} (h'(z) - g'(z)) ike^{ikz} e^{ikz} \mathrm{d}z \qquad \forall k \in (0, k_{\max}), \tag{69}$$

$$v_{k,1}(0) = \frac{-i}{\sqrt{2}k_1} \int_0^{+\infty} (h'(z) + g'(z)) ike^{ikz} e^{ik_1 z} \mathrm{d}z \qquad \forall k \in (\pi, k_{\max}). \tag{70}$$

We notice that

$$v_{k,0}(0) = 2ik\Gamma(h' - g')(2k) \qquad \forall k \in (0, k_{\max}), \tag{71}$$

$$v_{k,1}(0) = -\frac{\sqrt{2}ik(k_1 + k)}{k_1} \Gamma(h' + g')(k + k_1) \qquad \forall k \in (\pi, k_{\max}). \tag{72}$$

We define $s_0 = h' - g'$ and $s_1 = h' + g'$. We have access to $\Gamma(s_0)(k)$ for all $k \in (0, 2k_{\max})$, and since $k \mapsto k + \sqrt{k^2 - \pi^2}$ is one-to-one from $(\pi, k_{\max})$ to $(\pi, k_{\max} + \sqrt{k_{\max}^2 - \pi^2})$, we have access

to $\Gamma(s_1)(k)$ for all $k \in (\pi, k_{\max} + \sqrt{k_{\max}^2 - \pi^2})$. We denote by $d_0(k) = \Gamma(s_0)(k)$, $d_1(k) = \Gamma(s_1)(k)$ the data and consider the perturbed data $d_{0_{\text{app}}}$, $d_{1_{\text{app}}}$. We want to use the method described in section 2 to reconstruct $s_{0_{\text{app}}}$, $s_{1_{\text{app}}}$, an approximation of s_0, s_1. We can control the error of this approximation:

Proposition 28. Let $s_0, s_1, s_{0_{\text{app}}}, s_{1_{\text{app}}} \in \mathrm{H}^1(-r, r)$ where $r \in \mathbb{R}_+^*$. Let $k_{\max} \in R_+^*$, $d_0 = \Gamma(s_0)$, $d_{0_{\text{app}}} = \Gamma(s_{0_{\text{app}}})$ defined on $(0, 2k_{\max})$, $d_1 = \Gamma(s_1)$, $d_{1_{\text{app}}} = \Gamma(s_{1_{\text{app}}})$ defined on $(\pi, k_{\max} + \sqrt{k_{\max}^2 - \pi^2})$. Assume that there exists $M \in \mathbb{R}_+^*$ such that $\|s_i\|_{\mathrm{H}^1(-r,r)} \leq M$ and $\|s_{i_{\text{app}}}\|_{\mathrm{H}^1(-r,r)} \leq M$ for $i = 0, 1$. Then for every $\varepsilon \in \mathbb{R}_+^*$, $\varepsilon < 1$ there exists a constant $\xi_{k_{\max}}$ depending on r, M, ε such that

$$\|s_0 - s_{0_{\text{app}}}\|_{\mathrm{L}^2(-r,r)}^2 \leq \frac{4}{\pi}\|d_0 - d_{0_{\text{app}}}\|_{\mathrm{H}}^2 + \frac{2\pi}{k_{\max}^2} M^2, \tag{73}$$

$$\|s_1 - s_{1_{\text{app}}}\|_{\mathrm{L}^2(-r,r)}^2 \leq \xi_{k_{\max}}\|d_1 - d_{1_{\text{app}}}\|_{\mathrm{H}}^{2-2\varepsilon} + \frac{4}{\pi}\|d_1 - d_{1_{\text{app}}}\|_{\mathrm{H}}^2 + \frac{8\pi}{\left(k_{\max} + \sqrt{k_{\max}^2 - \pi^2}\right)^2} M^2. \tag{74}$$

Proof. We notice that $|\mathcal{F}(h')(k)| = 2|k\Gamma(h')(k)|$ and we use Theorem 22 and Remark 23 with $\omega_0 = 0$ and $\omega_1 = 2k_{\max}$, and then $\omega_0 = \pi$ and $\omega_1 = k_{\max} + \sqrt{k_{\max}^2 - \pi^2}$. □

Remark 29. This estimate highlights the different sources of error: the error due to the perturbed data, the error due to the lack of measurements at high frequencies, and errors due to the lack of measurements for the low frequencies of s_1.

Using the reconstruction of s_0 and s_1, we can find h' and g' and integrate them to find h and g. To conclude, with the measurements, on a section of the waveguide, of the scattered field associated with a source $\tilde{s}_k = -2ik\delta_0(x)$ for all the frequencies in $(0, k_{\max})$, we are able to reconstruct an approximation of h and g, the amplitude in the height of the waveguide. Moreover, we can quantify the error of this approximation, and this error diminishes if K increases and if the bump gets smaller.

3.4 Detection of inhomogeneities

This case is different from the two previous cases. A inhomogeneity affects the index of the medium and leads to changes in the homogeneous Helmholtz equation:

$$\Delta u + k^2(1 + h(x, y))u = 0. \tag{75}$$

We assume that $\mathrm{supp}(h)$ is compact and that the inhomogeneity is located to the right of the section $\{0\} \times (0, 1)$. To detect the defect, we introduce a source $s_k = -2ik\delta_0(x)$. Without any defect, the wave field generated by this source would be $u_k^{\text{inc}} := e^{ik|x|}$. Let u_k^s be the scattered wave field defined by $u_k^s := u_k - u_k^{\text{inc}}$. We know that u_k satisfies the equation (7), and so

$$\begin{cases} \Delta u_k^s + k^2 u_k^s = -k^2 h u_k^{\text{inc}} - k^2 h u_k^{\text{inc}} & \text{in } \Omega, \\ \partial_\nu u_k^s = 0 & \text{on } \partial\Omega, \\ u_k^s \text{ is outgoing.} \end{cases} \tag{76}$$

If we define $f(u) := k^2 h u$ then f satisfies the hypothesis of proposition 10 and for every $r > 0$,

$$\|f\|_{\mathcal{L}_c(\mathrm{H}^2(\Omega_r), \mathrm{L}^2(\Omega_r))} \leq k^2 \|h\|_{\mathrm{L}^\infty(-r,r)}. \tag{77}$$

Proposition 10 shows that if $k^2\|h\|_{\mathrm{L}^\infty(-r,r)}$ is small enough, u_k^s is close to v_k the solution of

$$\begin{cases} \Delta v_k + k^2 v_k = -k^2 h u_k^{\mathrm{inc}} & \text{in } \Omega, \\ \partial_\nu v_k = 0 & \text{on } \partial\Omega, \\ v_k \text{ is outgoing.} \end{cases} \tag{78}$$

and that with C the constant defined in Proposition 8,

$$\|u - v\|_{\mathrm{H}^2(-r,r)} \leq \frac{C^2 k^4 \|h\|^2_{\mathrm{L}^\infty(-r,r)} \|u_k^{\mathrm{inc}}\|_{\mathrm{L}^2(-r,r)}}{1 - Ck^2\|h\|_{\mathrm{L}^\infty(-r,r)}}. \tag{79}$$

We assume that the measurements consist in the n-th propagative mode $v_{k,n}$ for all frequencies $k \in (0, k_{\max})$ where $k_{\max} > 0$ is given. Using Proposition 3, we see that

$$v_{n,k}(0) = \frac{i}{2k_n} \int_0^{+\infty} k^2 h_n(z) e^{ikz} e^{ik_n z} \mathrm{d}z = \frac{(k+k_n)k^2}{k_n} \Gamma(h_n)(k+k_n) \quad \forall k \in (0, k_{\max}). \tag{80}$$

Since we assume that we are only able to measure the propagative modes, the frequency k must satisfy $k > n\pi$, and k_n is real. The function $k \mapsto k + \sqrt{k^2 - n^2\pi^2}$ is one-to-one from $(n\pi, k_{\max})$ to $(n\pi, k_{\max} + \sqrt{k_{\max}^2 - n^2\pi^2})$. This means that we have access to $\Gamma(h_n)(k)$ for every $k \in (n\pi, k_{\max} + \sqrt{k_{\max}^2 - n^2\pi^2})$. We denote by $d_n = \Gamma(h_n)$ the data and by $d_{n_{\mathrm{app}}}$ the perturbed data. We use the method described in section 2 to reconstruct $h_{n_{\mathrm{app}}}$, an approximation of h_n, and we can control the error of this approximation using Theorem 22.

Proposition 30. Let $n \in \mathbb{N}$, $h_{n_{\mathrm{app}}}, h_n \in \mathrm{H}^1(-r,r)$ where $r > 0$. Let $k_{\max} > n\pi$, $d_n(k) = \Gamma(h_n)(k)$ and $d_{n_{\mathrm{app}}}(k) = \Gamma(h_{n_{\mathrm{app}}})(k)$ for $k \in (n\pi, k_{\max} + \sqrt{k_{\max}^2 - n^2\pi^2})$. We assume that there exists $M \in \mathbb{R}_+^*$ such that $\|h_n\|_{\mathrm{H}^1(-r,r)} \leq M$ and $\|h_{n_{\mathrm{app}}}\|_{\mathrm{H}^1(-r,r)} \leq M$. Then for every $0 < \varepsilon < 1$ there exists a constant $\xi_{n,k_{\max}}$ depending on r, M, ε such that

$$\|h_n - h_{n_{\mathrm{app}}}\|^2_{\mathrm{L}^2(-r,r)} \leq \xi_{n,k_{\max}} \|d_n - d_{n_{\mathrm{app}}}\|^{2-2\varepsilon}_{\mathrm{H}} + \frac{4}{\pi}\|d_n - d_{n_{\mathrm{app}}}\|^2_{\mathrm{H}} + \frac{8\pi}{\left(k_{\max} + \sqrt{k_{\max}^2 - n^2\pi^2}\right)^2} M^2. \tag{81}$$

Corollary 31. Let $k_{\max} \in \mathbb{R}_+^*$ and $N \in \mathbb{N}$ such that $N < k_{\max}/\pi$. Let $h_{\mathrm{app}}, h \in \mathrm{H}^1(\Omega_r)$ where $r > 0$ and $d = F(h)$, $d_{\mathrm{app}} = F_s(h_{\mathrm{app}})$ such that d_n and $d_{n_{\mathrm{app}}}$ are defined on $(n\pi, k_{\max} + \sqrt{k_{\max}^2 - n^2\pi^2})$. We assume that there exists $M \in \mathbb{R}_+^*$ such that $\|h\|_{\mathrm{H}^1(\Omega_r)} \leq M$ and $\|h_{\mathrm{app}}\|_{\mathrm{H}^1(\Omega_r)} \leq M$. Then for every $0 < \varepsilon < 1$ there exists a constant $\xi_{N,k_{\max}}$ depending on r, M, ε such that

$$\|h - h_{\mathrm{app}}\|^2_{\mathrm{L}^2(\Omega_r)} \leq \xi_{N,k_{\max}} (N+1)^\varepsilon \|d - d_{\mathrm{app}}\|^{2-2\varepsilon}_{\ell^2(H)} + \frac{4}{\pi}\|d - d_{\mathrm{app}}\|^2_{\mathrm{l}^2(H)} + \frac{8\pi(N+1)}{K^2} M^2 + \frac{4}{N^2\pi^2} M^2. \tag{82}$$

Proof. Using the previous proposition,

$$\|h - h_{\mathrm{app}}\|^2_{\mathrm{L}^2(\Omega_r)} \leq \sum_{n=0}^{N} \xi_{n,k_{\max}} \|d_n - d_{n_{\mathrm{app}}}\|^{2-2\varepsilon}_{\mathrm{H}} + \frac{4}{\pi}\|d_n - d_{n_{\mathrm{app}}}\|^2_{\mathrm{H}} + \frac{8\pi M^2}{\left(k_{\max} + \sqrt{k_{\max}^2 - n^2\pi^2}\right)^2} + \sum_{n>N} \|h_n - h_{n_{\mathrm{app}}}\|^2_{\mathrm{L}^2(-r,r)}.$$

We define $\xi_{N,k_{\max}} = \max_{n=0,..,N} \xi_{n,k_{\max}}$ and using the concavity of $x \mapsto x^{1-\varepsilon}$, we deduce that

$$\|h - h_{\text{app}}\|^2_{\mathrm{L}^2(\Omega_r)} \leq \xi_{N,k_{\max}}(N+1)^{\varepsilon}\|d - d_{\text{app}}\|^{2-2\varepsilon}_{\ell^2(H)} + \frac{4}{\pi}\|d - d_{\text{app}}\|^2_{\ell^2(H)} + \frac{8\pi M^2(N+1)}{k^2_{\max}} + \frac{\|\partial_y(h - h_{\text{app}})\|^2_{\mathrm{L}^2(\Omega_r)}}{N^2\pi^2}.$$

We conclude using the upper bound on $\|h\|_{\mathrm{H}^1(\Omega_r)}$ and $\|h_{\text{app}}\|_{\mathrm{H}^1(\Omega_r)}$. □

Remark 32. This estimate highlights the different sources of error: the error due to the lack of measurements if the mode if greater than 1 in the low frequencies, the error due to the perturbed data, the error due to the lack of measurements in the high frequencies and finally the error due to the truncation to the N-th mode. The predominant term here seems to be the first one, and we need to find a balance between increasing N to decrease the error of truncation and diminishing N to lower the value of $\xi_{N,k_{\max}}$.

Unlike the two previous cases, the detection of inhomogeneities requires more modes than just the first two modes. However, using measurements on one section of the scattered field associated with a source $s_k = -2ik\delta_0(x)$, we are able to reconstruct an approximation of h and we can quantify the error made by this approximation.

4 Numerical Results

4.1 Numerical source inversion from limited frequency data

In Proposition 15 we have seen that the forward modal operator Γ is inversible. Knowing the measurements of the wavefield generated by a source for every frequencies, we are theoretically abble to reconstruct the source. Moreover, in Theorem 22, we have shown that if the source is compactly supported and satisfies some specific properties, we only need the measurements for a finite interval of frequencies to approximate the source. We now discuss the numerical aspects of such an inversion.

We assume that the wavefield in the waveguide is generated by a source f compactly supported, located between the sections $x = x_m$ and $x = x_M$. The interval $[x_m, x_M]$ is regularly discretized by a set of values X, and we want to find an approximation of $f(X)$. The measurements of the wavefield are made for a discrete set of frequencies denoted K. Let N_X and N_K be the length of X and K, we define $h = \frac{x_M}{N_X - 1}$ the stepsize for the discretization of X. Using Definition 14 and the operator Γ defined in (27), the operator $f \mapsto (k \mapsto k\Gamma(f)(k))$ maps $\mathrm{L}^2(\mathbb{R})$ onto $\mathrm{L}^2(\mathbb{R}^*_+)$ and can be discretized by the operator

$$\gamma : \begin{array}{ccc} \mathbb{C}^{N_X} & \to & \mathbb{C}^{N_K} \\ y & \mapsto & \left(\frac{ih}{2}\sum_{x\in X} y_x e^{ikx}\right)_{k\in K} \end{array}. \tag{83}$$

To invert this operator, we use a least square method. Given the data $d = \gamma(f(X))$, we want to find an approximation of $f(X)$ by minimizing the quantity

$$\frac{1}{2}\|\gamma(y) - d\|^2_{\ell^2(\mathbb{C}^{N_X})}.$$

To avoid small oscillations in the reconstruction we also define the discrete gradient

$$G : \begin{array}{ccc} \mathbb{C}^{N_X} & \to & \mathbb{C}^{N_X} \\ y & \mapsto & (y_i - y_{i-1})_{1\leq i\leq N_X} \end{array}, \tag{84}$$

with the convention that $x_0 = x_{N_X}$ and $x_{N_X+1} = x_1$. Note that the adjoints of γ and G can be easily computed. For $\lambda > 0$, we now try to minimize the quantity

$$J(y) = \frac{1}{2}\|\gamma(y) - d\|^2_{\ell^2(\mathbb{C}^{N_K})} + \frac{\lambda}{2}\|G(y)\|^2_{\ell^2(\mathbb{C}^{N_X})}. \tag{85}$$

To this end, we use the steepest descent method, with the initialization $y_0 = (0)_{x\in X}$, which reads

$$y_{m+1} = y_m - \frac{\|\nabla J(y_m)\|^2_{\ell^2(\mathbb{C}^{N_X})}}{\|S(\nabla J(y_m))\|^2_{\ell^2(\mathbb{C}^{N_K})} + \|G(\nabla J(y_m))\|^2_{\ell^2(\mathbb{C}^{N_X})}}\nabla J(y_m). \tag{86}$$

We use this algorithm to illustrate the results given in Theorem 22. First, we reconstruct a source f with a gap in the high frequencies, meaning that we have access to the measurements of the wavefield generated by f for a discret set of frequencies between 0 and ω_1. In figure 5, we present the comparison between a function f and its reconstruction for different values of ω_1. As expected, we observe convergence when ω_1 increases, and the reconstruction becomes almost perfect visually.

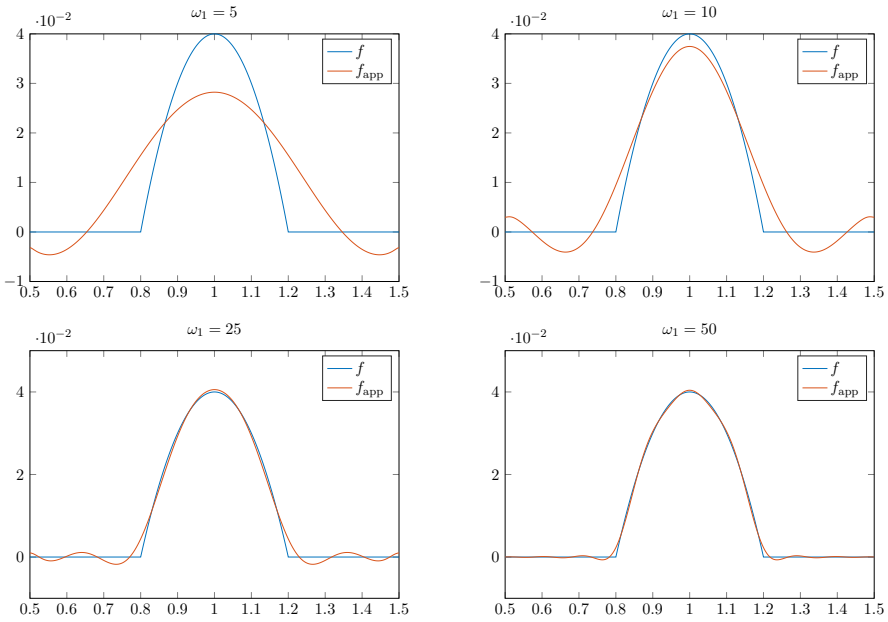

Figure 5: Reconstruction of $f(x) = (x - 0.8)(1.2 - x)\mathbf{1}_{0.8\leq x\leq 1.2}$ for different values of ω_1 using the discrete operator γ and the algorithm (86) with $\lambda = 0.001$. Here, X is the discretization of $[0.5, 1.5]$ with 251 points, and K is the discretization of $[0.01, \omega_1]$ with 1000 points.

Secondly, we investigate the influence of r and ω_0 in Theorem 22. Consistently with Propositions 28 and 30, we choose ω_0 to be a multiple of π. In figure 6, we present the comparison between a 1D function f and its reconstruction for different values of ω_0 when the support of f is fixed. In figure 7, we present the comparison between a 1D function f and its reconstruction for different sizes r of

support when ω_0 is fixed. As expected from the definition of the constant C of the Thorem 22, the quality of the reconstruction deteriorates when r and ω_0 increase.

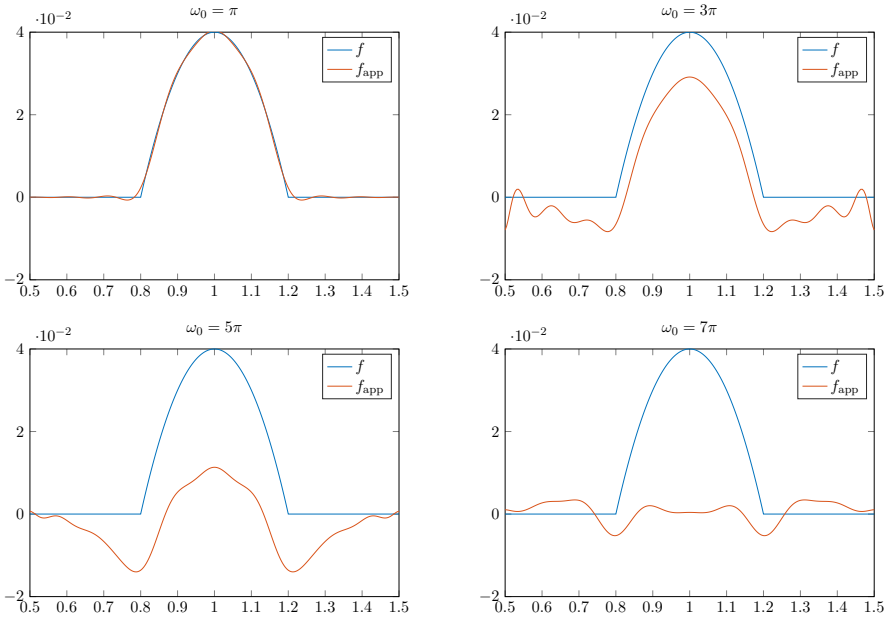

Figure 6: Reconstruction of $f(x) = (x-0.8)(1.2-x)\mathbf{1}_{0.8\leq x\leq 1.2}$ for different values of ω_0 and $r = 0.5$ using the discrete operator γ and the algorithm (86) with $\lambda = 0.001$. Here, X is the discretization of $[0.5, 1.5]$ with 251 points, and K is the discretization of $[\omega_0, 50]$ with 1000 points.

To conclude, the reconstruction for source is almost perfect for $\omega_0 = 0$ if we increase sufficiently ω_1. However, if $\omega_0 > 0$, the problem is ill-conditioned and if the size of the support of the source or ω_0 increase, the reconstruction does not fit well the source.

4.2 Generation of data for the detection of defects

In order to apply the results of section 3 to reconstruct defects, we need to have access to the measurements generated by the defect on a section of the wavefield . To generate this data, we use the software Matlab to solve numerically the equation satisfied by the wavefield in the waveguide, and to evaluate its solution on a section. The equations of propagation in a regular waveguide Ω are given respectively for a bend, a bump and a inhomogeneity by (59), (67) and (76). In the following, we assume that the interesting part of the waveguide is located between $x = 0$ and $x = 8$, and that the measurements are made on the section $\{1\} \times (0, 1)$. To generate the solution of these equations of propagation on $[0, 8] \times [0, 1]$, we use the finite element method and a perfectly matched layer on the left side of the waveguide between $x = -19$ and $x = 0$ and on the right side between $x = 8$ and $x = 27$. The coefficient of absorption for the perfectly matched layer is defined by $-k((x-8)\mathbf{1}_{x\geq 8} - x\mathbf{1}_{x\leq 0})$. The structured mesh is built with a stepsize of $0,01$.

4.3 Detection of bends

Using the method described in the previous subsection, we generate the solution of (59) for a set of frequencies K and we evaluate the solutions on the section $\{1\} \times (0, 1)$. As explained in section 3.2

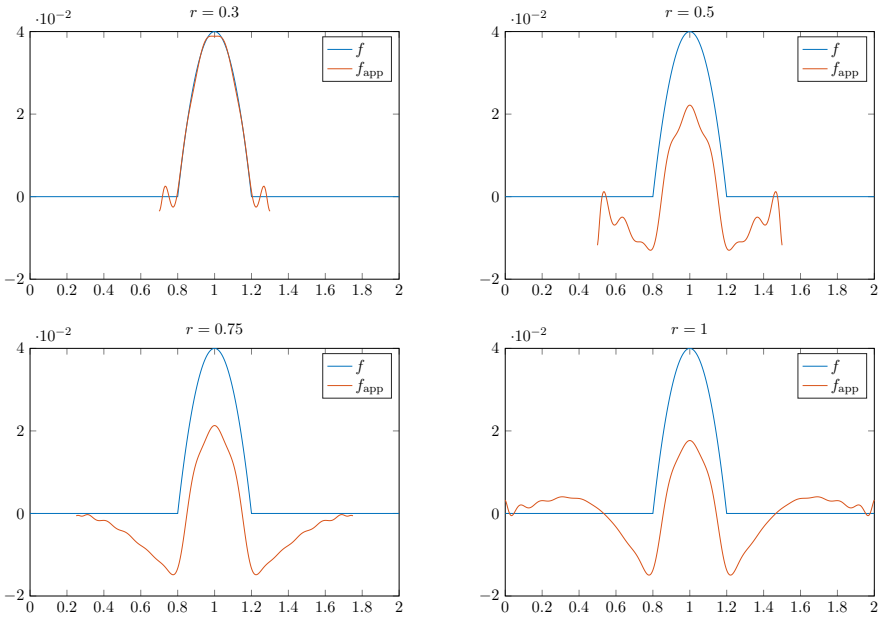

Figure 7: Reconstruction of $f(x) = (x - 0.8)(1.2 - x)\mathbf{1}_{0.8 \leq x \leq 1.2}$ for different sizes of support r and $\omega_0 = 3\pi$ using the discrete operator γ and the algorithm (86) with $\lambda = 0.001$. Here, X is the discretization of $[1 - r, 1 + r]$ with $500r + 1$ points, and K is the discretization of $[3\pi, 50]$ with 1000 points.

and equation (62), the corresponding data tantamount to knowing $\Gamma(s)(2k)$ for every $k \in K$, where

$$s = \mathbf{1}_{x \in [x_c, x_c + \theta(r+1)]} \left(1 - \frac{1}{2(r+1)} - (r+1) \ln \left(\frac{r+1}{r} \right) \right). \tag{87}$$

Using this data, we want to find an approximation s_{app} of s. We could use the algorithm (86) to obtain this approximation. However, since we know that we are looking for a rectangular function, we can directly define $s_{\text{app}} = -p_1 \mathbf{1}_{x \in [p_2, p_2 + p_3]}$ and see that

$$\Gamma(s_{\text{app}})(k) = -\frac{ip_1}{k} e^{ik\frac{2p_2+p_3}{2}} \sin\left(\frac{p_3}{2} k \right). \tag{88}$$

We find (p_1, p_2, p_3) by minimizing $\|\Gamma(s_{\text{app}})(2k) - \Gamma(s)(2k)\|_{\ell^2(\mathbb{C}^{N_K})}$, and the approximations of x_c, r and θ follow. We present in Figure 8 the reconstruction of two different bends, and in Table 1 the relative error on the estimation of (x_c, r, θ) for different bends. We can see that if the bend is really small, the reconstruction is very good. On the other hand, when r increases or when θ decreases, the reconstruction deteriorates due to the fact that the Born approximation is no longer a good approximation of the wavefield in the waveguide.

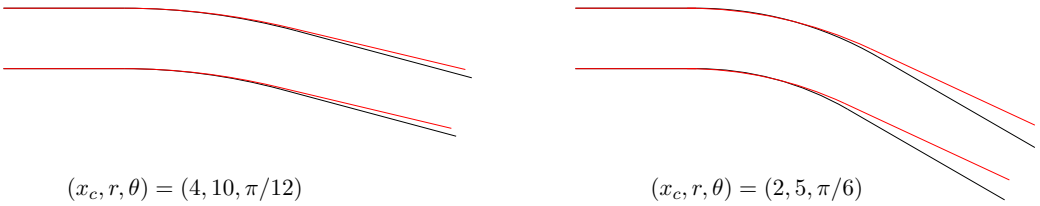

$(x_c, r, \theta) = (4, 10, \pi/12)$ $(x_c, r, \theta) = (2, 5, \pi/6)$

Figure 8: Reconstruction of two different bends. The black lines represent the initial shape of Ω, and the red the reconstruction of Ω. In both cases, K is the discretization of $[0.01, 40]$ with 100 points, and the reconstruction is obtain by (88). On the left, the initial parameters of the bend are $(x_c, r, \theta) = (4, 10, \pi/12)$ and on the right, $(x_c, r, \theta) = (2, 5, \pi/6)$.

(x_c, r, θ)	$(2.5, 40, \pi/80)$	$(4, 10, \pi/12)$	$(2, 5, \pi/6)$
relative error on x_c	1.8%	0%	7.6%
relative error on r	3.0%	7.5%	23.8%
relative error on θ	1.6%	10.7%	16.9%

Table 1: Relative errors on the reconstruction of (x_c, r, θ) for different bends. In each case, K is the discretization of $[0.01, 40]$ with 100 points, and the reconstruction is obtain by (88).

4.4 Detection of bumps

Using the method described in section 4.2, we generate the solutions of (67) for a set of frequencies K and we evaluate the solutions on the section $\{1\} \times (0, 1)$. Using Remark 6, and to ensure that the Born hypothesis (18) is satisfied, we do not choose any frequencies in $[n\pi - 0.2, n\pi + 0.2]$ for every $n \in \mathbb{N}$. As explained in section 3.3 and equations (71), (72), the data only determines $\Gamma(s_0)(2k)$ for every $k \in K$ and $\Gamma(s_1)(k + \sqrt{k^2 - \pi^2})$ for every $k \in K$, $k > \pi$, where h and g paramatrize the bump and $s_0 = h' + g'$, $s_1 = -\sqrt{2}h' + g'$. Using the algorithm (86), we find an approximation of h' and g', and then by integration the approximation of h and g follows. In figure 9, we represent two different reconstructions of a shape defect. As predicted in Proposition 25, the reconstruction improves when $\|h\|_{\mathcal{C}^1(\mathbb{R})}$ and $\|g\|_{\mathcal{C}^1(\mathbb{R})}$ decrease. Table 2 illustrates this point as it depicts the relative error on a reconstruction of h when its amplitude increases.

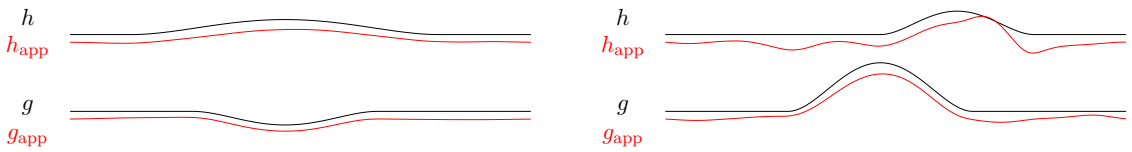

Figure 9: Reconstruction of two shape defects. In black, the initial shape of Ω, and in red the reconstruction, slightly shifted for comparison purposes. In both cases, K is the discretization of $[0.01, 70] \setminus \{[n\pi - 0.2, n\pi + 0.2], n \in \mathbb{N}\}$ with 300 points, X is the discretization of $[3, 4.5]$ with 151 points and we use the algorithm (86) with $\lambda = 0.08$ to reconstruct s_0 and s_1. On the left, $h(x) = \frac{5}{16}\mathbf{1}_{3.2 \leq x \leq 4.2}(x - 3.2)^2(4.2 - x)^2$ and $g(x) = -\frac{35}{16}\mathbf{1}_{3.4 \leq x \leq 4}(x - 3.4)^2(4 - x)^2$. On the right, $h(x) = \frac{125}{16}\mathbf{1}_{3.7 \leq x \leq 4.2}(x - 3.7)^2(4.2 - x)^2$ and $g(x) = \frac{125}{16}\mathbf{1}_{3.4 \leq x \leq 4}(x - 3.4)^2(4 - x)^2$.

A	0.1	0.2	0.3	0.5
$\|h - h_{\text{app}}\|_{\mathrm{L}^2(\mathbb{R})} / \|h\|_{\mathrm{L}^2(\mathbb{R})}$	8.82%	10.41%	15.12%	54.99%

Table 2: Relative errors on the reconstruction of h for different amplitudes A. We choose $h(x) = A\mathbf{1}_{3\leq x\leq 5}(x-3)^2(5-x)^2$ and $g(x) = 0$. In every reconstruction, K is the discretization of $[0.01, 40] \setminus \{[n\pi - 0.2, n\pi + 0.2], n \in \mathbb{N}\}$ with 100 points, X is the discretization of $[1, 7]$ with 601 points and we use the algorithm (86) with $\lambda = 0.08$ to reconstruct h'.

4.5 Detection of inhomogeneities

Using the method described in section 4.2, we generate the solutions of (76) for a set of frequencies K and we evaluate the solutions on the section $\{1\} \times (0, 1)$. As explained in section 3.4 and equation (80), the data only determines $\Gamma(h_n)(k + k_n)$ for every $k \in K$, $k > n\pi$ where h_n is the n-th mode of h, and h is the inhomogeneity. We define a number of modes N used for the recontruction of h, and with the algorithm (86), we find an approximation of h_n for every $n \leq N$. In Figure 10, we show the reconstruction of h_n for $0 \leq n \leq N = 9$. We obtain an approximation of h by using the expression $h(x, y) = \sum_{n\in\mathbb{N}} h_n(x)\varphi_n(y)$. In Figures 11 and 12 we present two reconstructions of h. In the first one, h has a small support and is very well reconstructed. In the second one, the support of h is larger. Even if the latter reconstruction does not yield a good approximation of h, it allows localization of the inhomogeneities in the waveguide. Moreover, if we assume that h is a positive function, we can improve the algorithm (86) by reconstructing h on each step and projecting on the space of positive functions (see the third part of Figure 12).

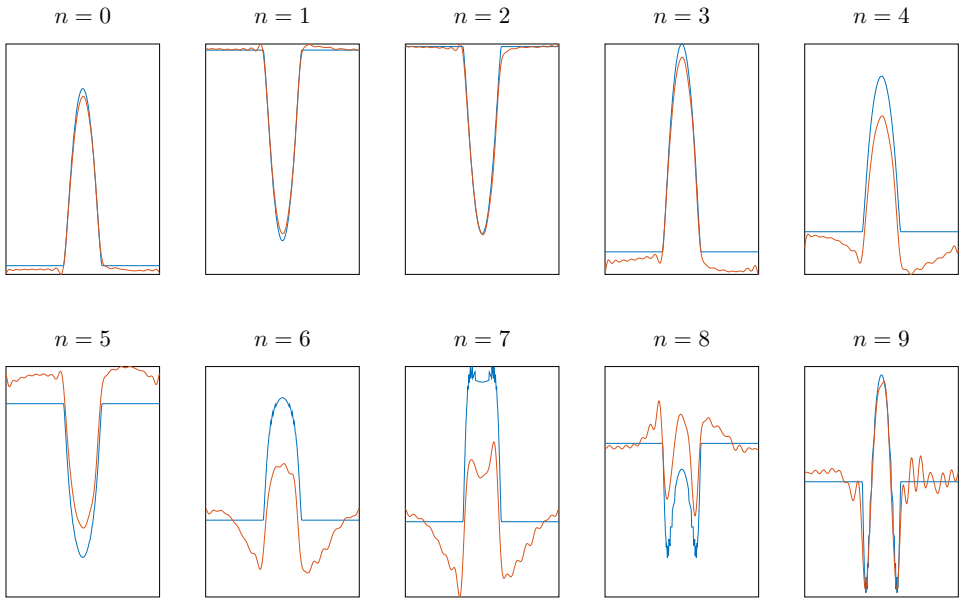

Figure 10: Recontruction of h_n for $0 \leq n \leq 9$, where $h(x) = 0.05\mathbf{1}_{|(\frac{x-4}{0.05}, \frac{y-0.6}{0.15})|\leq 1} \left|\left(\frac{x-4}{0.05}, \frac{y-0.6}{0.15}\right)\right|^2$. In blue, we represent h_n and in red the reconstruction of $h_{n_{\text{app}}}$. In every reconstruction, K is the discretization of $[0.01, 150]$ with 200 points, X is the discretization of $[3.8, 4.2]$ with 101 points and we use the algorithm (86) with $\lambda = 0.002$ to reconstruct every h_n.

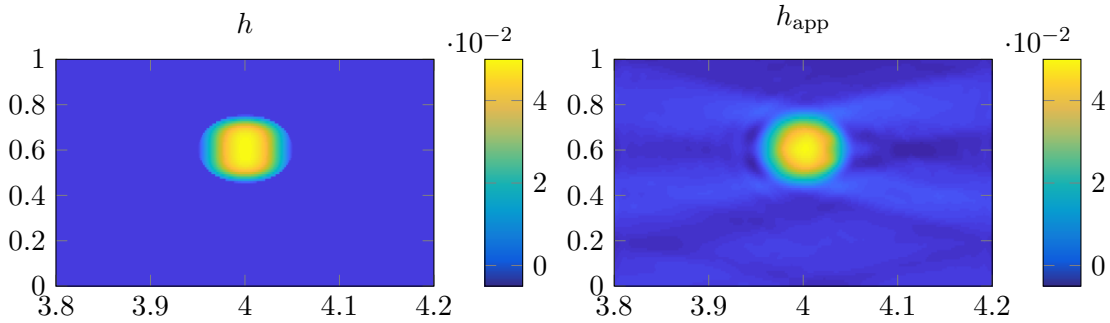

Figure 11: Recontruction of h where $h(x) = 0.05\mathbf{1}_{|(\frac{x-4}{0.05}, \frac{y-0.6}{0.15})|\leq 1} \left|\left(\frac{x-4}{0.05}, \frac{y-0.6}{0.15}\right)\right|^2$. On the left, we represent the initial shape of h, and on the right the reconstruction h_{app}. Here, K is the discretization of $[0.01, 150]$ with 200 points, X is the discretization of $[3.8, 4.2]$ with 101 points and we use the algorithm (86) with $\lambda = 0.002$ to reconstruct every h_n. We used $N = 20$ modes to reconstruct h.

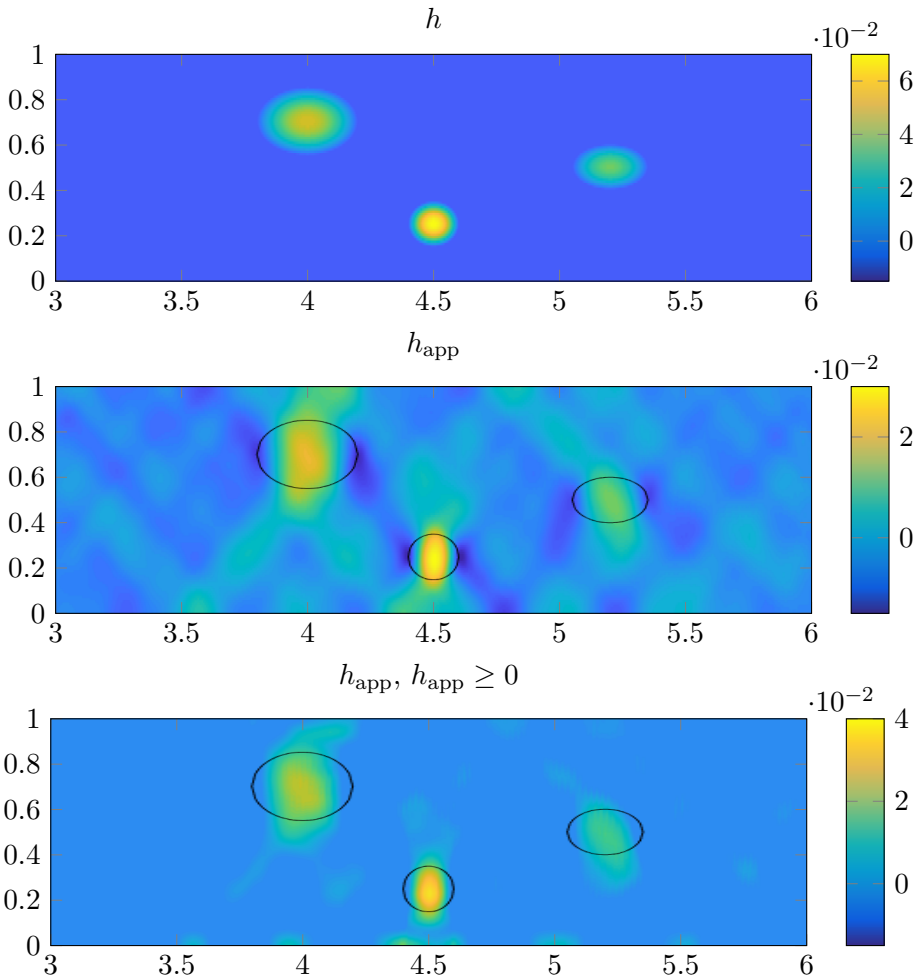

Figure 12: Recontruction of an inhomogeneity h. From top to bottom, the initial representation of h, the reconstruction h_{app} and the reconstruction h_{app} with the knowledge of the positivity of h. Here, K is the discretization of $[0.01, 150]$ with 200 points, X is the discretization of $[3, 6]$ with 3001 points and we use the algorithm (86) with $\lambda = 0.01$ to reconstruct every h_n. We choose used $N = 20$ modes to reconstruct h.

5 Conclusion

In this paper, we present a new approach to recover defects in a waveguide. By sending the first propagative mode for frequencies in a given interval, we measure the scattered wave field generated by the defects on a slice of the waveguide. Using the properties of the Fourier transform and the Born approximation, we propose a method to reconstruct the parameters of the defect. We provide a control of the error made in the approximation of the parameters if the defects are "small" enough so that the Born approximation makes sense

Our numerical results show that the method works well for the three types of defects considered : bends, bumps, localized inhomogeneities. Using a finite element method to generate the measurements, we were able to recover numerically different types of small defects using the modal decomposition and a penalized least square algorithm. Our reconstruction of inhomogeneities are similar to the one presented in [10], and while they can increase the number of propagative mode sent in the waveguide to improve the reconstruction, we can increase the number of frequencies we use.

This work could be extended to other types of defects such as impenetrable obstacles or cracks in the waveguide. One could also try to apply this multi-frequency point of view to elastic waveguides, where a modal decomposition in Lamb waves is also available.

Appendix A: Proof of Proposition 3 and 7

We begin with the proof of proposition 3. Let $r > 0$, $\Omega_r = (-r, r) \times (0, 1)$ and T the application defined by

$$T : \begin{array}{ccc} \mathrm{L}^2(\Omega_r) & \to & \mathrm{L}^2(-r,r)^{\mathbb{N}} \\ u & \mapsto & \left(\displaystyle\int_0^1 u(x,y)\varphi_n(y)\mathrm{d}y \right)_{n\in\mathbb{N}} \end{array}.$$

Let H_1 be the Hilbert space

$$\mathrm{H}_1 := \left\{ (u_n) \in \ell^2(\mathrm{H}^1(-r,r)), \sum_{n\in\mathbb{N}} n^2 \|u_n\|^2_{\mathrm{L}^2(-r,r)} < +\infty \right\},$$

with the scalar product

$$\langle (u_n), (v_n) \rangle_{\mathrm{H}_1} = \sum_{n\in\mathbb{N}} (1 + n^2\pi^2) \langle u_n, v_n \rangle_{\mathrm{L}^2(-r,r)} + \sum_{n\in\mathbb{N}} \langle u_n', v_n' \rangle_{\mathrm{L}^2(-r,r)}.$$

The application T is an Hilbert isomorphism between $\mathrm{H}^1(\Omega_r)$ and H_1.

We first try and find a solution to (7). If we rewrite the problem in a variational formulation, for every $v \in \mathrm{H}^1(\Omega_r)$,

$$\int_{\Omega_r} \nabla u_k \nabla v - k^2 \int_{\Omega_r} u_k v = \int_{\Omega_r} sv. \tag{89}$$

Using the isomorphism T, we write that $T(u_k) = (u_{k,n})_{n\in\mathbb{N}}$, $T(v) = (v_n)_{n\in\mathbb{N}}$, and we notice that this variational formulation is equivalent to the sequence of problems

$$\forall v_n \in \mathrm{H}^1(-r,r), \qquad \int_{-r}^{r} u_{k,n}' v_n' + (n^2\pi^2 - k^2) \int_{-r}^{r} u_{k,n} v_n = \int_{-r}^{r} s_n v_n. \tag{90}$$

Setting $k_n^2 = k^2 - n^2\pi^2$ with $\mathrm{Re}(k_n) > 0$, $\mathrm{Im}(k_n) > 0$, this variation formulation is associated to the equation $u''_{k,n} + k_n^2 u_{k,n} = s_n$. We notice that $G_{k_n}(x) = \frac{i}{2k_n} e^{ik_n|x|}$ satisfies the equation $G''_{k_n} + k_n^2 G_{k_n} = -\delta_0$ and so we define $u_k := T^{-1}\left((G_{k_n} * s_n)_{n\in\mathbb{N}}\right)$. Using this definition, $u_k \in \mathrm{H}^1(\Omega_r)$ and satisfies (89). Moreover, u_k is outgoing. Finaly, using results from the elliptical regularity (see [13]) we deduce that $u_k \in \mathrm{H}^2(\Omega_r)$. Since this result holds for every $r > 0$, we conclude that $u_k \in \mathrm{H}^2_{\mathrm{loc}}(\Omega)$.

We find the solution of (11) using the same method. The variational formulation gives for every $v \in \mathrm{H}^1(\Omega_r)$,

$$\int_{\Omega_r} \nabla u_k \nabla v - k^2 \int_{\Omega_r} u_k v - \int_{\Omega_{\mathrm{top}}} b_1 v - \int_{\Omega_{\mathrm{bot}}} b_2 v = 0. \tag{91}$$

Using the isomorphim T, this formulation is equivalent for every $n \in \mathbb{N}$ to

$$\int_{-r}^{r} u'_{k,n} v'_n + (n^2\pi^2 - k^2) \int_{-r}^{r} u_{k,n} v_n = \int_{-r}^{r} (b_1 \varphi_n(1) + b_2 \varphi_n(0)) v_n.$$

Then, we define $u_k := T^{-1}\left((G_{k_n} * (b_1\varphi_n(1) + b_2\varphi_n(0)))_{n\in\mathbb{N}}\right)$ and again u_k is in $\mathrm{H}^1(\Omega_r)$, is outgoing and satisfies (91). Using the elliptical regularity, we deduce that $u_k \in \mathrm{H}^2(\Omega_r)$.

To prove uniqueness for both problems, we notice that u_k satisfies $\Delta u_k + k^2 u_k = 0$ in Ω. Thus, u_k is a classical solution in $\mathcal{C}^\infty(\Omega)$ and can be written as a linear combination of $(x, y) \mapsto \varphi_n(y) e^{\pm i k_n x}$. But since u_k is outgoing, it leads to $u_k = 0$.

Appendix B: Proof of Proposition 5 and 8

We begin with the proof of proposition 5. Using the same notation as in Appendix A, the function G_{k_n} satisfies

$$\|G_{k_n}\|_{\mathrm{L}^1(-2r,2r)} \leq \begin{cases} \frac{2r}{k_n} & \text{if } n < k/\pi, \\ \frac{1}{|k_n|} \min\left(\frac{1}{|k_n|}, 2r\right) & \text{if } n > k/\pi, \end{cases}$$

$$\|G'_{k_n}\|_{\mathrm{L}^1(-2r,2r)} \leq \begin{cases} 2r & \text{if } n < k/\pi, \\ \min\left(\frac{1}{|k_n|}, 2r\right) & \text{if } n > k/\pi. \end{cases}$$

We define $\delta = \min_{n\in\mathbb{N}}\left(\sqrt{|k^2 - n^2\pi^2|}\right)$, and we apply the Young inequality to $u_{k,n}$:

$$\|u_{k,n}\|_{\mathrm{L}^2(-r,r)} \leq \|G_{k_n}\|_{\mathrm{L}^1(-2r,2r)} \|s_n\|_{\mathrm{L}^2(-r,r)}.$$

It leads to

$$\|u_k\|^2_{\mathrm{L}^2(\Omega_r)} \leq \frac{4r^2}{\delta^2} \sum_{n\in\mathbb{N}} \|s_n\|^2_{\mathrm{L}^2(-r,r)} = \frac{4r^2}{\delta^2} \|s\|^2_{\mathrm{L}^2(\Omega_r)}.$$

Applying the Young inequality to $u'_{k,n}$, we get

$$\|\nabla u_k\|^2_{\mathrm{L}^2(\Omega_r)} \leq 4r^2 \sum_{n<k/\pi} \left(1 + \frac{n^2\pi^2}{k_n^2}\right) \|s_n\|^2_{\mathrm{L}^2(-r,r)} + 4r^2 \sum_{n>k/\pi} \left(1 + \frac{n^2\pi^2}{|k_n|^2}\right) \|s_n\|^2_{\mathrm{L}^2(-r,r)}.$$

If N is the largest propagative mode, then if $n > k/\pi > N$,

$$1 + \frac{n^2\pi^2}{|k_n|^2} \leq 1 + \frac{(N+1)^2\pi^2}{|k_{N+1}|^2} \leq 1 + \frac{(N+1)^2\pi^2}{\delta^2}.$$

It leads to

$$\|\nabla u_k\|^2_{\mathrm{L}^2(\Omega_r)} \leq 4r^2 \left(1 + \frac{(k+\pi)^2}{\delta^2}\right) \|s\|^2_{\mathrm{L}^2(\Omega_r)}.$$

Finally, we notice that

$$\|\nabla^2 u_k\|^2_{\mathrm{L}^2(\Omega_r)} = \sum_{n\in\mathbb{N}} n^4\pi^4 \|u_{k,n}\|^2_{\mathrm{L}^2(-r,r)} + \sum_{n\in\mathbb{N}} 2n^2\pi^2 \|u'_{k,n}\|^2_{\mathrm{L}^2(-r,r)} + \sum_{n\in\mathbb{N}} \|u''_{k,n}\|^2_{\mathrm{L}^2(-r,r)},$$

and that

$$\|u''_{k,n}\|^2_{\mathrm{L}^2(-r,r)} = \| - s_n - k_n^2 u_{k,n}\|^2_{\mathrm{L}^2(-r,r)} \leq \left(\|s_n\|_{\mathrm{L}^2(-r,r)} + k_n^2 \|u_{k,n}\|_{\mathrm{L}^2(-r,r)}\right)^2.$$

Combining both relations yields

$$\begin{aligned}\|\nabla^2 u\|^2_{\mathrm{L}^2(\Omega_r)} \leq \sum_{n<k/\pi} &\left(\frac{4r^2n^4\pi^4}{k_n^2} + 8n^2\pi^2r^2 + (1+2k_nr)^2\right) \|s_n\|^2_{\mathrm{L}^2(-r,r)} \\ &+ \sum_{n>k/\pi} \left[\frac{n^4\pi^4}{|k_n|^4} + \frac{2n^2\pi^2}{|k_n|^2} + \left(1 + \frac{|k_n|^2}{|k_n|} \min\left(\frac{1}{|k_n|}, 2r\right)\right)^2\right] \|s_n\|^2_{\mathrm{L}^2(-r,r)}.\end{aligned}$$

If N is the largest propagative mode, then if $n > k/\pi$,

$$\frac{n^4\pi^4 \min\left(\frac{1}{|k_n|^2}, 4r^2\right)}{|k_n|^2} + 2n^2\pi^2 \min\left(\frac{1}{|k_n|^2}, 4r^2\right) \leq \frac{(k+\pi)^4}{\delta^4} + 2\frac{(k+\pi)^2}{\delta^2},$$

and the following estimate holds

$$\|\nabla^2 u\|^2_{\mathrm{L}^2(\Omega_r)} \leq \left[\max\left(4r^2, \frac{1}{\delta^2}\right)\left(\frac{(k+\pi)^4}{\delta^2} + 2(k+\pi)^2\right) + \max((1+2kr)^2, 4)\right] \|s\|^2_{\mathrm{L}^2(\Omega_r)}.$$

To prove Proposition 8, we deduce from the results in [13] that there exist a constant $d(r)$ and $\mu > 0$ such that

$$\|u_k\|_{\mathrm{H}^2(\Omega_r)} \leq d(r)\left(\| - \Delta u_k + \mu u_k\|_{\mathrm{L}^2(\Omega_r)} + \|b_1\|_{\mathrm{H}^{1/2}(-r,r)} + \|b_2\|_{\mathrm{H}^{1/2}(-r,r)}\right),$$

and if follows that

$$\|u\|_{\mathrm{H}^2(\Omega_r)} \leq d(r)\left((k^2+\mu)\|u\|_{\mathrm{L}^2(\Omega_r)} + \|b_1\|_{\mathrm{H}^{1/2}(-r,r)} + \|b_2\|_{\mathrm{H}^{1/2}(-r,r)}\right).$$

Using the same method as for the estimation of $\|u_{k,n}\|_{\mathrm{L}^2(-r,r)}$ with the Young inequality, we get

$$\|u\|^2_{\mathrm{L}^2(\Omega_r)} \leq \left(\|b_1\|^2_{\mathrm{H}^{1/2}(-r,r)} + \|b_2\|^2_{\mathrm{H}^2 1/2(-r,r)}\right)\left(\sum_{n<k/\pi} \frac{4r^2}{k_n^2} + \sum_{n>k/\pi} \frac{1}{k_n^4}\right).$$

Finally, we see that

$$D = d(r)\left((k^2+\mu)\max\left(2r, \frac{1}{\delta}\right)\sqrt{\sum_{n\in\mathbb{N}} \frac{1}{k_n^2}} + 1\right).$$

References

[1] L. Abrahamsson, Orthogonal grid generation for two-dimensional ducts, *Journal of Computational and Applied Mathematics*, **34** (1991), 305 – 314.

[2] L. Abrahamsson and H. O. Kreiss, Numerical solution of the coupled mode equations in duct acoustics, *Journal of Computational Physics*, **111** (1994), 1 – 14.

[3] H. Ammari, E. Iakovleva and H. Kang, Reconstruction of a small inclusion in a two-dimensional open waveguide, *SIAM Journal on Applied Mathematics*, **65** (2005), 2107–2127.

[4] G. Bao and F. Triki, Reconstruction of a defect in an open waveguide, *Science China Mathematics*, **56** (2013), 2539–2548.

[5] J. P. Berenger, A perfectly matched layer for the absorption of electromagnetic waves, *Journal of Computational Physics*, **114** (1994), 185–200.

[6] L. Bourgeois and S. Fliss, On the identification of defects in a periodic waveguide from far field data, *Inverse Problems*, **30**.

[7] L. Bourgeois and E. Lunéville, The linear sampling method in a waveguide: A modal formulation, *Inverse Problems*, **24**.

[8] D. Colton and A. Kirsch, A simple method for solving inverse scattering problems in the resonance region, *Inverse Problems*, **12** (1996), 383–393.

[9] D. Colton and R. Kress, *Inverse Acoustic and Electromagnetic Scattering Theory*, Applied Mathematical Sciences, Springer Berlin Heidelberg, 1997.

[10] S. Dediu and J. R. McLaughlin, Recovering inhomogeneities in a waveguide using eigensystem decomposition, *Inverse Problems*, **22** (2006), 1227–1246.

[11] A. S. B.-B. Dhia, L. Chesnel and S. A. Nazarov, Perfect transmission invisibility for waveguides with sound hard walls, *Journal de Mathématiques Pures et Appliquées*, **111** (2018), 79 – 105.

[12] H. Dym and H. P. McKean, *Fourier series and integrals*, Academic Press New York, 1972.

[13] P. Grisvard, *Elliptic Problems in Nonsmooth Domains*, Society for Industrial and Applied Mathematics, 2011.

[14] M. Kharrat, O. Bareille, W. Zhou and M. Ichchou, Nondestructive assessment of plastic elbows using torsional waves: Numerical and experimental investigations, *Journal of Nondestructive Evaluation*, **35** (2016), 1–14.

[15] M. Kharrat, M. N. Ichchou, O. Bareille and W. Zhou, Pipeline inspection using a torsional guided-waves inspection system. part 1: Defect identification, *International Journal of Applied Mechanics*, **6**.

[16] Y. Y. Lu, Exact one-way methods for acoustic waveguides, *Mathematics and Computers in Simulation*, **50** (1999), 377 – 391.

[17] W. McLean, *Strongly Elliptic Systems and Boundary Integral Equations*, Cambridge University Press, 2000.

[18] J. Todd, The condition number of the finite segment of the hilbert matrix, *National Bureau of Standarts, Applied Mathematics Series*, 109–119.